

AD-A057 416

HONEYWELL INC HOPKINS MINN
MINI-REFRACTION SONDE LABORATORY TESTS.(U)
DEC 77 C D MOTCHENBACHER

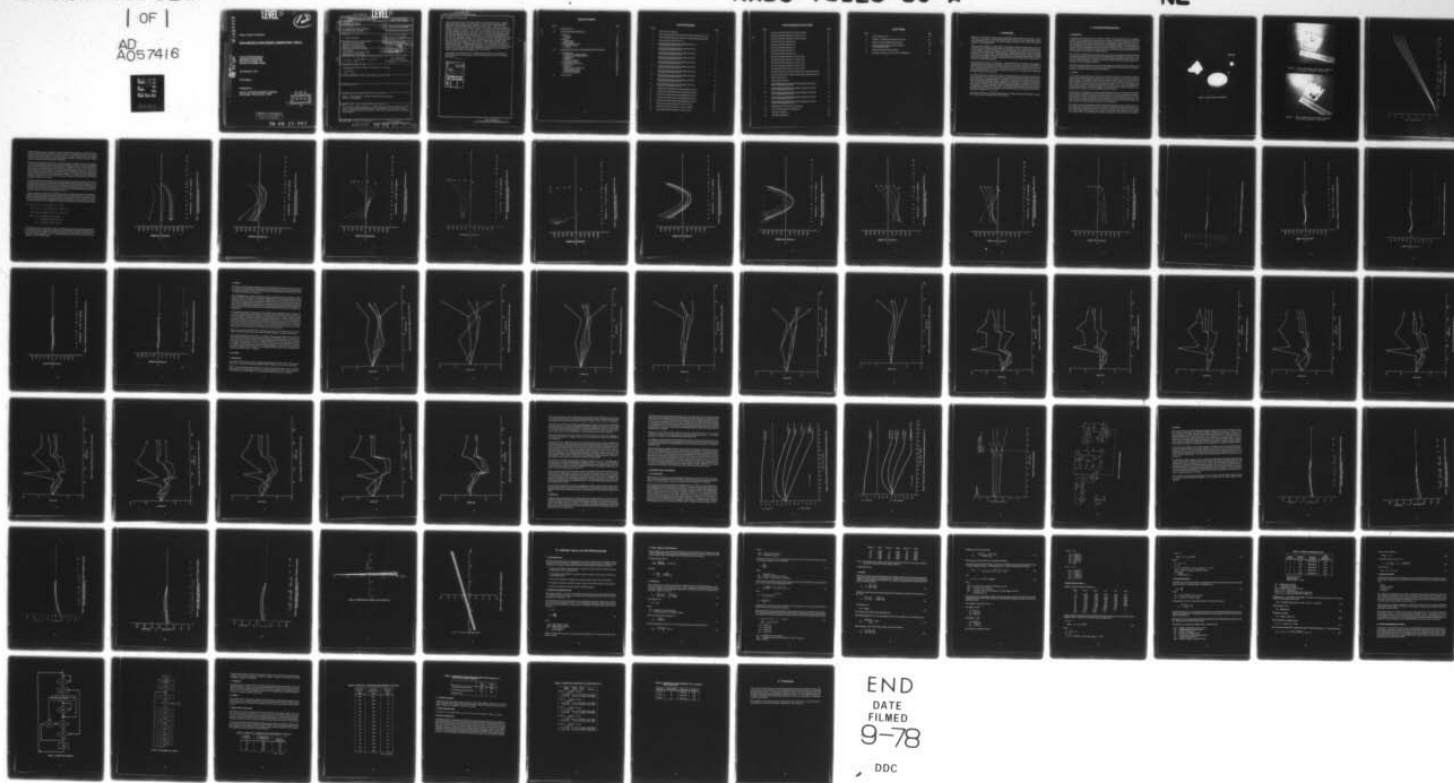
F/G 4/2

UNCLASSIFIED

| OF |
AD
A057416

NADC-76128-30-A

N62269-76-C-0368
NL



LEVEL II

2
(12)

AD A057416

Report NADC-76129-30-A

MINI-REFRACTION SONDE LABORATORY TESTS

**AD No. 1
DDC FILE COPY**

Curtis D. Motchenbacher
Honeywell Incorporated
600 Second Street, N.E.
Hopkins, Minnesota 55343

30 December 1977

Final Report

Prepared for

NAVAL AIR DEVELOPMENT CENTER
Warminster, Pennsylvania 18974

DDC
RECEIVED
AUG 15 1978
RECEIVED
D

DISTRIBUTION STATEMENT A

Approved for public release;
Distribution Unlimited

78 08 11 001

UNCLASSIFIED

LEVEL II

SECURITY CLASSIFICATION OF THIS PAGE (When Data Entered)

19 REPORT DOCUMENTATION PAGE		READ INSTRUCTIONS BEFORE COMPLETING FORM	
1 REPORT NUMBER	2 GOVT ACCESSION NO.	3 RECIPIENT'S CATALOG NUMBER	
16 NADC-76128-30-A			
4 TITLE (and Subtitle)		5 TYPE OF REPORT & PERIOD COVERED	
6 MINI-REFRACTION SONDE LABORATORY TESTS.		9 Final Summary Report.	
7 AUTHOR(s)		6 PERFORMING ORG REPORT NUMBER	
C. Motchenbacher			
9 PERFORMING ORGANIZATION NAME AND ADDRESS		8 CONTRACT OR GRANT NUMBER(s)	
Honeywell Incorporated 600 Second Street, N. E. Hopkins, Minnesota 55343		15 N62269-76-C-0368/P00001	
11 CONTROLLING OFFICE NAME AND ADDRESS		10 PROGRAM ELEMENT PROJECT, TASK AREA & WORK UNIT NUMBERS	
Commander Naval Air Development Center Warminster, Pa. 18974		62759N F52-551 WF52551734 RG701	
14 MONITORING AGENCY NAME & ADDRESS (if different from Controlling Office)		12 REPORT DATE	
10 Curt's D./Motchenbacher		11 30 December 1977	
		13 NUMBER OF PAGES	
		73	
		15 SECURITY CLASS (of this report)	
		UNCLASSIFIED	
		15a DECLASSIFICATION DOWNGRADING SCHEDULE	
16 DISTRIBUTION STATEMENT (of this Report)			
Approved for Public Release; Distribution Unlimited. 12 76p.			
17 DISTRIBUTION STATEMENT (of the abstract entered in Block 20, if different from Report)			
18 SUPPLEMENTARY NOTES			
19 KEY WORDS (Continue on reverse side if necessary and identify by block number)			
Sonde, Meteorological, Balloon, Barometer, Hygristor, Battery Transmitter			
20 ABSTRACT (Continue on reverse side if necessary and identify by block number)			
The purpose of this program is to demonstrate that it is feasible to build a small, lightweight meteorological sonde capable of measuring index of refraction (Mini-Refracton Sonde), which can be launched with a 30-gram Pibal balloon.			

DD FORM 1473

1 JAN 73

EDITION OF 1 NOV 65 IS OBSOLETE

UNCLASSIFIED

SECURITY CLASSIFICATION OF THIS PAGE (When Data Entered)

170 170

78 08

11

001LB

UNCLASSIFIED

SECURITY CLASSIFICATION OF THIS PAGE(When Data Entered)

20. ABSTRACT (Continued)

This minisonde uses a rod thermister for temperature and a carbon hygistor for humidity measurement. For pressure measurement, a Honeywell silicon diaphragm barometer was used. This pressure sensor consists of a small silicon chip with strain-sensitive resistors diffused into the surface. This sensor is mounted on an evacuated tube so that changes in absolute pressure can be measured. To commute between the temperature, pressure, and humidity sensors and encode the meteorological data measurements, a set of meteorological electronics was developed using commercially available integrated circuits. By use of integrated circuits, it is possible to achieve all the commutation functions in a small and particularly lightweight package. The sensors are commutated on a time basis, with a complete cycle every 400 milliseconds. A lightweight telemetry transmitter providing an output of 1/2 watt at 400 to 406 megahertz was designed and constructed. Power for the transmitter and minisonde electronics is provided by a small lithium battery consisting of 5-1/2 A cells.

Laboratory measurements in a temperature and pressure chamber demonstrate an rms accuracy of 0.5°C temperature and 0.8 millibar pressure.

ABSTRACT for	
NTIS	White Section <input checked="" type="checkbox"/>
DDC	Buff Section <input type="checkbox"/>
UNPROCESSED	<input type="checkbox"/>
JUSTIFICATION	
BY	
DISTRIBUTION/AVAILABILITY CODE	
Gen.	AVAIL. and/or SPECIAL
A	

UNCLASSIFIED

SECURITY CLASSIFICATION OF THIS PAGE(When Data Entered)

Table of Contents

Section	Page
I INTRODUCTION	1
II COMPONENT MEASUREMENTS	2
A. Barometer	2
1. Accuracy	22
2. Stability	22
B. Battery	22
1. Requirements	39
2. Battery Life	40
C. Meteorological Electronics	40
1. Circuit Description	45
2. Linearity	53
III LABORATORY TESTS ON THE MINI-REFRACTIONSONDES	53
A. Data Reduction	53
1. Frequency-to-Voltage Conversion	54
2. Supply Voltage and High Reference	54
3. Temperature	56
4. Humidity	59
5. Pressure and Altitude	61
6. Reduction Procedure	61
B. Sonde Measurement Accuracy	64
1. Temperature	64
2. Pressure	64
3. Effect of Airflow on Barometer	66
4. Telemetry Transmitter	66
5. Sonde Calibration Data	66
6. Balloon Characteristics	69
IV CONCLUSIONS	69

List of Illustrations

Figure		Page
1	Silicon Pressure Transducer	3
2	Silicon Diaphragm Barometer Mounted on Ceramic Substrate, Front View	4
3	Silicon Diaphragm Barometer Mounted on Ceramic Substrate, Back View	4
4	Barometer Output Signal (Unit No. 1)	5
5	Plots of Pressure Deviation from a Straight Line Fit over Temperature and Pressure (Unit 1)	7
6	Plots of Pressure Deviation from a Straight Line Fit over Temperature and Pressure (Unit 2)	8
7	Plots of Pressure Deviation from a Straight Line Fit over Temperature and Pressure (Unit 3)	9
8	Plots of Pressure Deviation from a Straight Line Fit over Temperature and Pressure (Unit 4)	10
9	Plots of Pressure Deviation from a Straight Line Fit over Temperature and Pressure (Unit 5)	11
10	Plots of Pressure Deviation from a Straight Line Fit over Temperature and Pressure (Unit 6)	12
11	Plots of Pressure Deviation from a Straight Line Fit over Temperature and Pressure (Unit 7)	13
12	Plots of Pressure Deviation from a Straight Line Fit over Temperature and Pressure (Unit 8)	14
13	Plots of Pressure Deviation from a Straight Line Fit over Temperature and Pressure (Unit 9)	15
14	Plots of Pressure Deviation from a Straight Line Fit over Temperature and Pressure (Unit 10)	16
15	Verification of the Barometer Linearizing Equation (Unit 1)	17
16	Verification of the Barometer Linearizing Equation (Unit 2)	18
17	Verification of the Barometer Linearizing Equation (Unit 3)	19
18	Verification of the Barometer Linearizing Equation (Unit 4)	20
19	Verification of the Barometer Linearizing Equation (Unit 5)	21
20	Barometer Drift Data (1000 mB, 0°C, S/N's 1,2,3,4,5)	23
21	Barometer Drift Data (1000 mB, 0°C, S/N's 6,7,8,9,10)	24
22	Barometer Drift Data (600 mB, 0°C, S/N's 1,2,3,4,5)	25

List of Illustrations (Concluded)

Figure		Page
23	Barometer Drift Data (600 mB, 0°C, S/N's 6,7,8,9,10)	26
24	Barometer Drift Data (200 mB, 0°C, S/N's 1,2,3,4,5)	27
25	Barometer Drift Data (200 mB, 0°C, S/N's 6,7,8,9,10)	28
26	Barometer Drift Data (1000 mB, 0°C)	29
27	Barometer Drift Data (900 mB, 0°C)	30
28	Barometer Drift Data (800 mB, 0°C)	31
29	Barometer Drift Data (700 mB, 0°C)	32
30	Barometer Drift Data (600 mB, 0°C)	33
31	Barometer Drift Data (500 mB, 0°C, S/N's 2,3,4,9)	34
32	Barometer Drift Data (400 mB, 0°C, S/N's 2,3,4,9)	35
33	Barometer Drift Data (300 mB, 0°C, S/N's 2,3,4,9)	36
37	Barometer Drift Data (200 mB, 0°C, S/N's 2,3,4,9)	37
35	Barometer Drift Data (100 mB, 0°C, S/N's 2,3,4,9)	38
36	Honeywell G3060 Lithium Cell Life Characteristics (Starting from 80°F)	41
37	Honeywell G3060 Lithium Cell Life Characteristics (Starting from 32°F)	42
38	Battery Characteristics	43
39	Meteorological Electronics	44
40	Shows Linearity of the Minisonde Voltage to Frequency Conversion for Five Final Models (Unit No. 7)	46
41	Shows Linearity of the Minisonde Voltage to Frequency Conversion for Five Final Models (Unit No. 8)	47
42	Shows Linearity of the Minisonde Voltage to Frequency Conversion for Five Final Models (Unit No. 9)	48
43	Shows Linearity of the Minisonde Voltage to Frequency Conversion for Five Final Models (Unit No. 10)	49
44	Shows Linearity of the Minisonde Voltage to Frequency Conversion for Five Final Models (Unit No. 11)	50
45	High Reference Stability versus Temperature	51
46	Supply Voltage Change with Temperature	52
47	Digitizer Flow Diagram	62
48	Data Reduction Sequence	63

List of Tables

Table		Page
1	Sonde Calibration Data	60
2	Sonde No. 7 Temperature Measurement Accuracy	64
3	Sonde No. 7 Pressure Measurement Accuracy	65
4	Barometric Pressure Measured with Sonde No. 8 with and without Airflow	66
5	Minisonde Telemetry Transmitter Data	67
6	Measured Characteristics of a 30-Gram Pibal Balloon	68

I. Introduction

The Navy has a requirement to measure the vertical profile of index of refraction from sea level to above 15,000 feet. It is necessary to make these measurements from many sizes and classes of ships. Further, these measurements must be made under typical operating conditions of calm or high winds and from stopped to full operational speed.

The purpose of this program is to demonstrate that it is feasible to build a small, lightweight meteorological sonde capable of measuring index of refraction (Mini-Refraction Sonde), which can be launched with a 30-inch diameter, 30-gram pibal balloon. In many field applications, it is difficult to fill and launch a very large balloon, either because of space limitations or because of high winds or other environmental conditions. It is very useful to have a balloon no larger than 30 inches in diameter so that it can be filled within a room and carried out through a standard ship's door for launching. Tests show that a 30-gram latex balloon, when inflated to 30 inches in diameter, will lift a 100-gram minisonde, including battery, at an ascent rate of 800 feet per minute.

During the previous section of this program, it was demonstrated that a 100-gram sonde capable of measuring temperature, pressure and humidity could be built. This minisonde used a rod thermistor for temperature and a carbon hygrometer for humidity measurement. For pressure measurement, a Honeywell silicon diaphragm barometer was used. This pressure sensor consists of a small silicon chip with strain-sensitive resistors diffused into the surface. This sensor is mounted on an evacuated tube so that changes in absolute pressure can be measured.

To commutate between the temperature, pressure, and humidity sensors and encode the meteorological data measurements, a set of meteorological electronics was developed using commercially available integrated circuits. By use of integrated circuits, it is possible to achieve all the commutation functions in a small and particularly lightweight package. The sensors are commutated on a time basis, with a complete cycle every 400 milliseconds. At a rise rate of 1,000 feet per minute, this gives a complete set of data every 7 feet of altitude. A special lightweight telemetry transmitter providing an output of 1/2 watt at 400 to 406 megahertz was designed and constructed by the Honeywell Defense Electronics Division (DEL-D), Annapolis, Maryland. Power for the transmitter and minisonde electronics was provided by a small lithium battery consisting of 5-1/2 AA cells.

The purpose of this section of the development program is to build five additional Mini-Refraction Sondes and to make laboratory measurements of their accuracy.

II. Component Measurements

A. BAROMETER

To determine the altitude of a sonde, it is necessary to make a continuous measurement of the atmospheric pressure. This is typically done with some form of a barometer. Honeywell manufactures a solid state pressure transducer fabricated from single crystal silicon. The pressure transducer sensor consists of a silicon chip that has been etched from the back to leave a thin diaphragm of silicon. The strain-sensitive resistors are diffused into the surface of the silicon to measure changes in deflection. The silicon diaphragm is mounted on an evacuated glass tube for absolute pressure measurement. Figure 1 is a photograph of the transducer element; the element on the right shows the top view of the silicon chip, the transducer on the left has a plastic cover protecting the sensing element.

When the silicon diaphragm chip is mounted on an evacuated tube, the diaphragm is deflected downward by atmospheric pressure. This causes a strain in the sensing resistors and changes their resistance. As the barometric pressure changes, the resistance of the sensors changes proportionately. Since the silicon resistors are temperature-sensitive as well as strain-sensitive, they are used in a bridge configuration to compensate for the temperature sensitivity.

The pressure transducers used in these tests were incorporated onto a thick film amplifier substrate that provides a calibrated amplification of the pressure signal. The thick film electronics also incorporates a thermistor temperature sensor for additional compensation.

1. Accuracy

To accurately measure pressure over the life of the sonde, the barometer must be both accurate and stable. Accuracy implies the ability to read a given voltage and translate it into the correct pressure. Stability implies the capability of retaining this accuracy over a period of time. For the Mini-Refraction Sonde application it is desirable to have an accuracy and a long term stability on the order of ± 0.1 percent, which is 1 millibar of accuracy over the temperature range of -50 to $+50^{\circ}\text{C}$. The purpose of this task is to demonstrate that the pressure transducer has an inherent accuracy and stability required by the Mini-Refraction Sonde. As will be demonstrated, the transducers have an accuracy of better than ± 1 millibar and are capable of a long term stability of about 1 millibar.

Figures 2 and 3 are photographs of the silicon diaphragm pressure transducer. The integrated amplifier and temperature compensation network are shown mounted on the ceramic substrate containing the thick film resistor elements. The barometer chip in Figure 2 is shown in the right-hand corner of the substrate. In Figure 3, the vacuum chamber tube for the barometer is seen in the upper left-hand corner. The light spots on the substrate resistors are caused by the automatic, computer controlled trimming of the resistor elements to adjust the span and sensitivity of the transducer.

The linearity of the silicon diaphragm pressure transducer is illustrated in Figure 4, which shows the output voltage versus input pressure for one pressure transducer. Note that the output is linear from 150 to past 1,050 millibars. The span or sensitivity, as well as the null offset, can be adjusted as desired during the manufacturing process to produce any sensitivity or range desired. These sensors are set to operate over a range of 150 to 1,050 millibars and to produce an output of 6 volts at full scale. For the Mini-

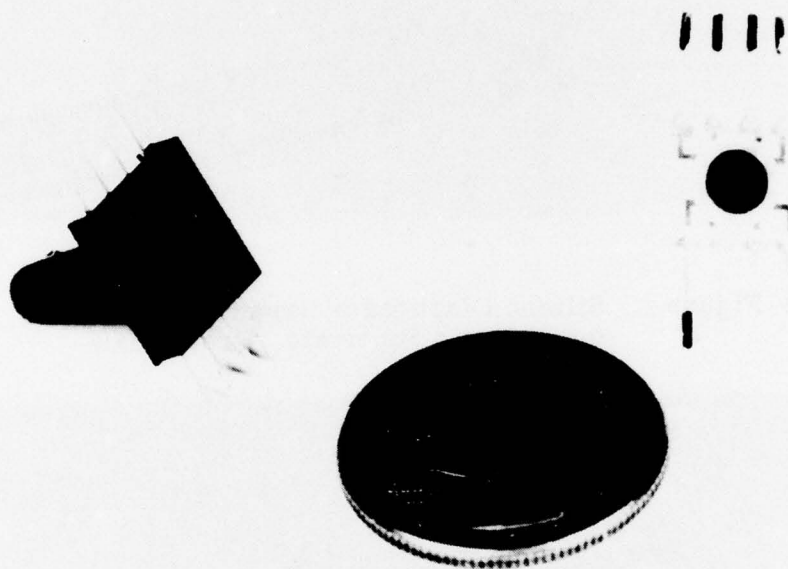


Figure 1. Silicon Pressure Transducer

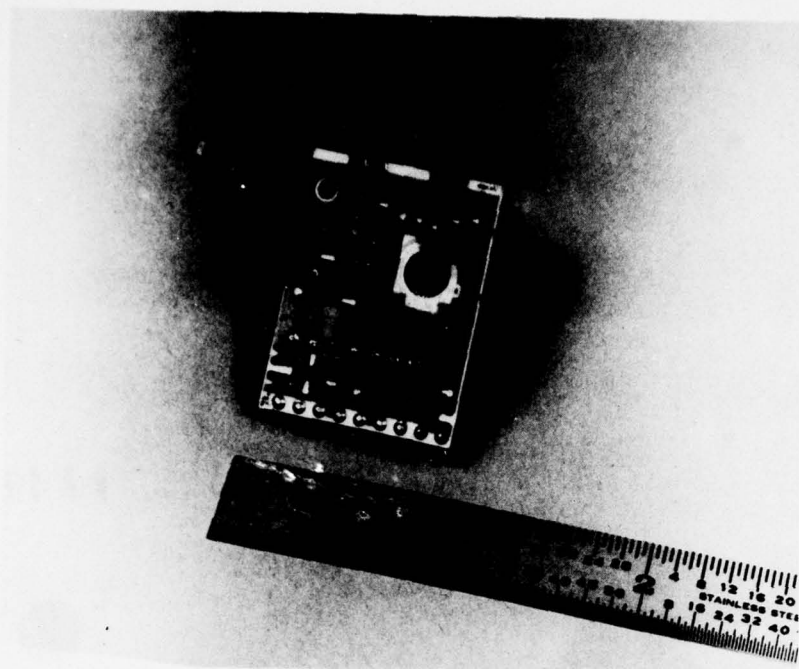


Figure 2. Silicon Diaphragm Barometer Mounted on Ceramic Substrate, Front View

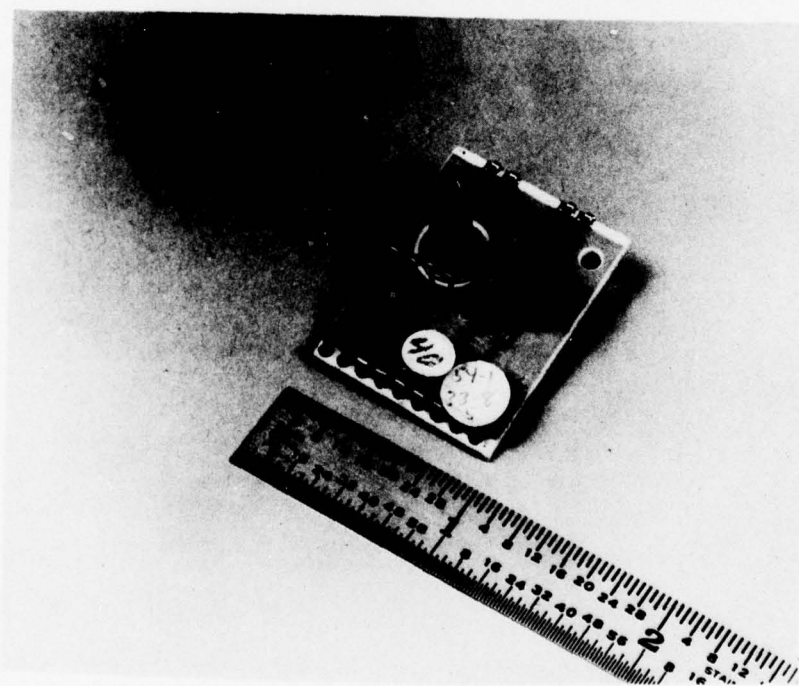


Figure 3. Silicon Diaphragm Barometer Mounted on Ceramic Substrate, Back View

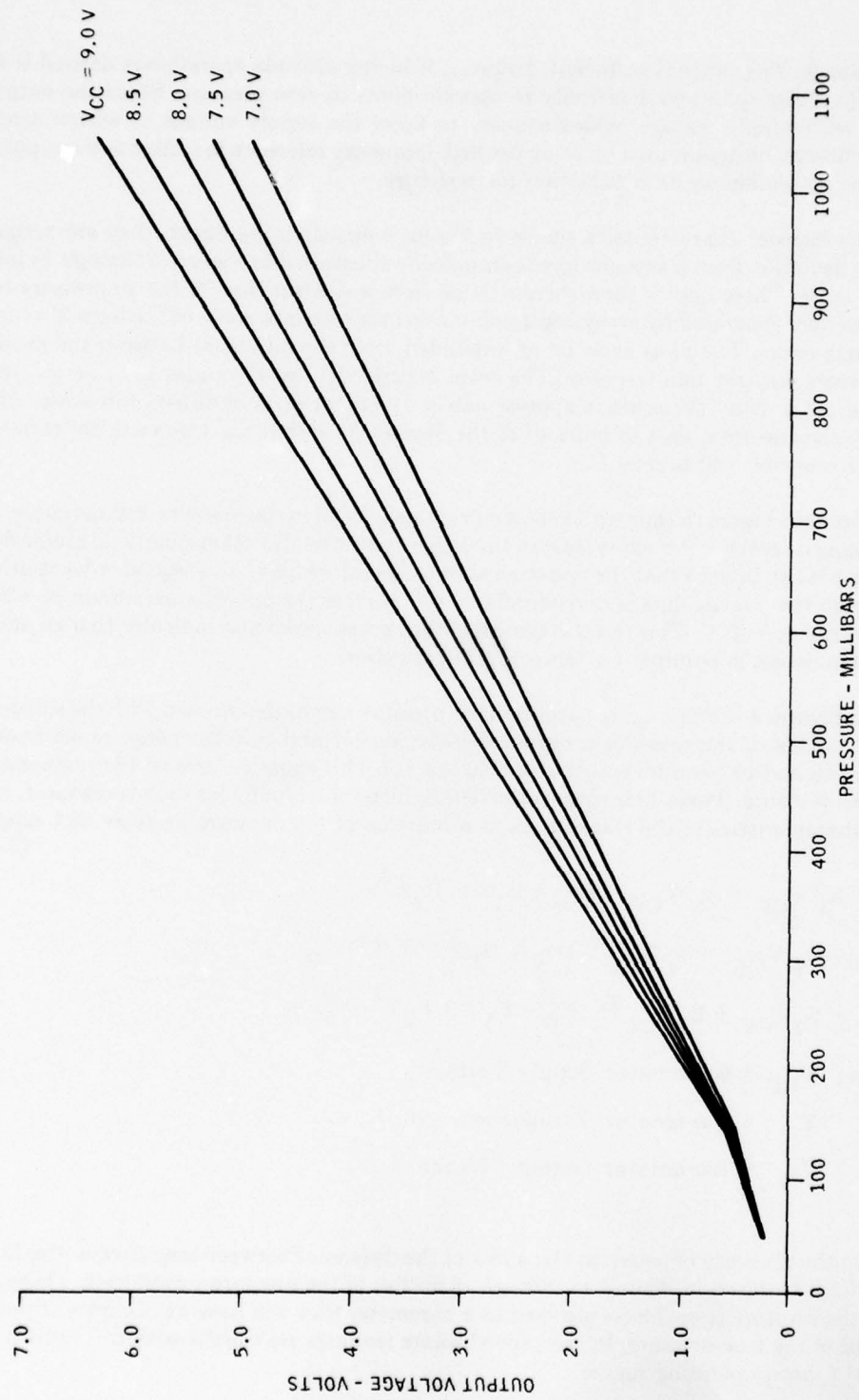


Figure 4. Barometer Output Signal (Unit No. 1)

Refraction Sonde, this range is sufficient; however, if higher altitude operation is desired it will be necessary to adjust the span and sensitivity to operate down to zero pressure. Since the output signal is ratiometric with supply voltage, it is necessary to know the supply voltage to within a few hundred millivolts. This can be determined by using the high frequency reference to calibrate the supply voltage as described in the section on data reduction methodology.

Although the transfer characteristics shown in Figure 4 appear to be linear, they are actually slightly curved. The deviation from a straight line is graphically illustrated in Figures 5 through 14 by expanding the vertical scale. These figures show the deviation from a straight line for the 10 pressure transducers. These curves were generated by assuming a nominal sensor response curve of the form $V = mP$ for 8-volt supply voltage curve. The plots show on an expanded scale the difference between the measured value and the average straight line response. The scale is expanded by 100 times to bring out the variation between the units. Note the scale is approximately 1 percent or 10 millibars full scale. Although the nonlinearity changes from unit to unit, all of the devices fit within the 1 percent limits over the entire temperature range of -40 to $+50^\circ\text{C}$.

All of the curves in Figures 5 through 14 show a prominent bend in the pressure-voltage curve. This can be corrected using a second order expression in the pressure transfer function equation. Similarly, if you observe Figure 5 it can be seen that the variation with temperature also has a second order relationship. The deviation from the straight line is maximum at -40° , reaches the opposite maximum at $+35^\circ$ and then continues to rise at $+50^\circ\text{C}$. This trend is typical of the curves shown and indicates that an additional second order expression is required for temperature correction

As shown in Figures 4 through 14, the atmospheric pressure can be determined with the silicon diaphragm pressure transducer if the transducer output voltage, supply and chip temperature are known. The expression for calculating pressure is shown in equation (1). This equation uses an 18 constant expression to calculate the pressure. These 18 constants are determined individually for each transducer, by use of the measured characteristics of the transducers as a function of temperature pressure and supply voltage.

$$P = (A_0 + A_1 V_{CC} + A_2 V_{CC}^2) (B_0 + B_1 T + B_2 T^2) + (C_0 + C_1 V_{CC} + C_2 V_{CC}^2) (D_0 + D_1 T + D_2 T^2) V_B + (E_0 + E_1 V_{CC} + E_2 V_{CC}^2) (F_0 + F_1 T + F_2 T^2) V_B^2 \quad (1)$$

where: V_{CC} = Barometer Supply Voltage
 T = Barometer Temperature in $^\circ\text{K}$
 V_B = Barometer Output Voltage

To illustrate the accuracy of equation (1), a plot of the difference between measured and calculated barometric readings is shown in Figures 15 through 19 for five of the pressure transducers. These curves show that when the pressure transducers are used as a barometer they will have an accuracy of well within ± 1 millibar rms of the true pressure. In fact, the absolute readings are usually within 1 millibar over supply voltage and typical operating ranges.

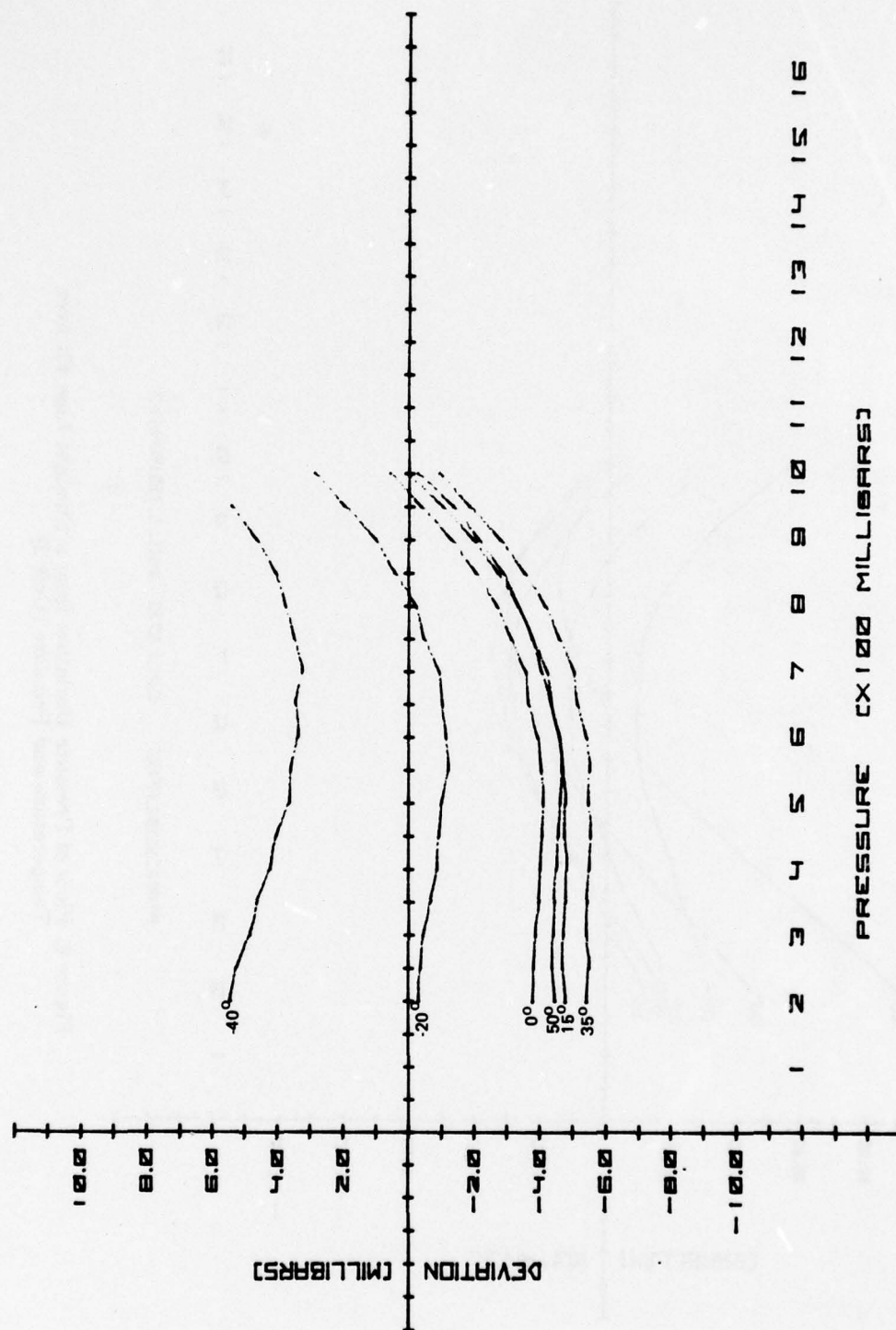


Figure 5. Plots of Pressure Deviation from a Straight Line Fit over Temperature and Pressure (Unit 1)

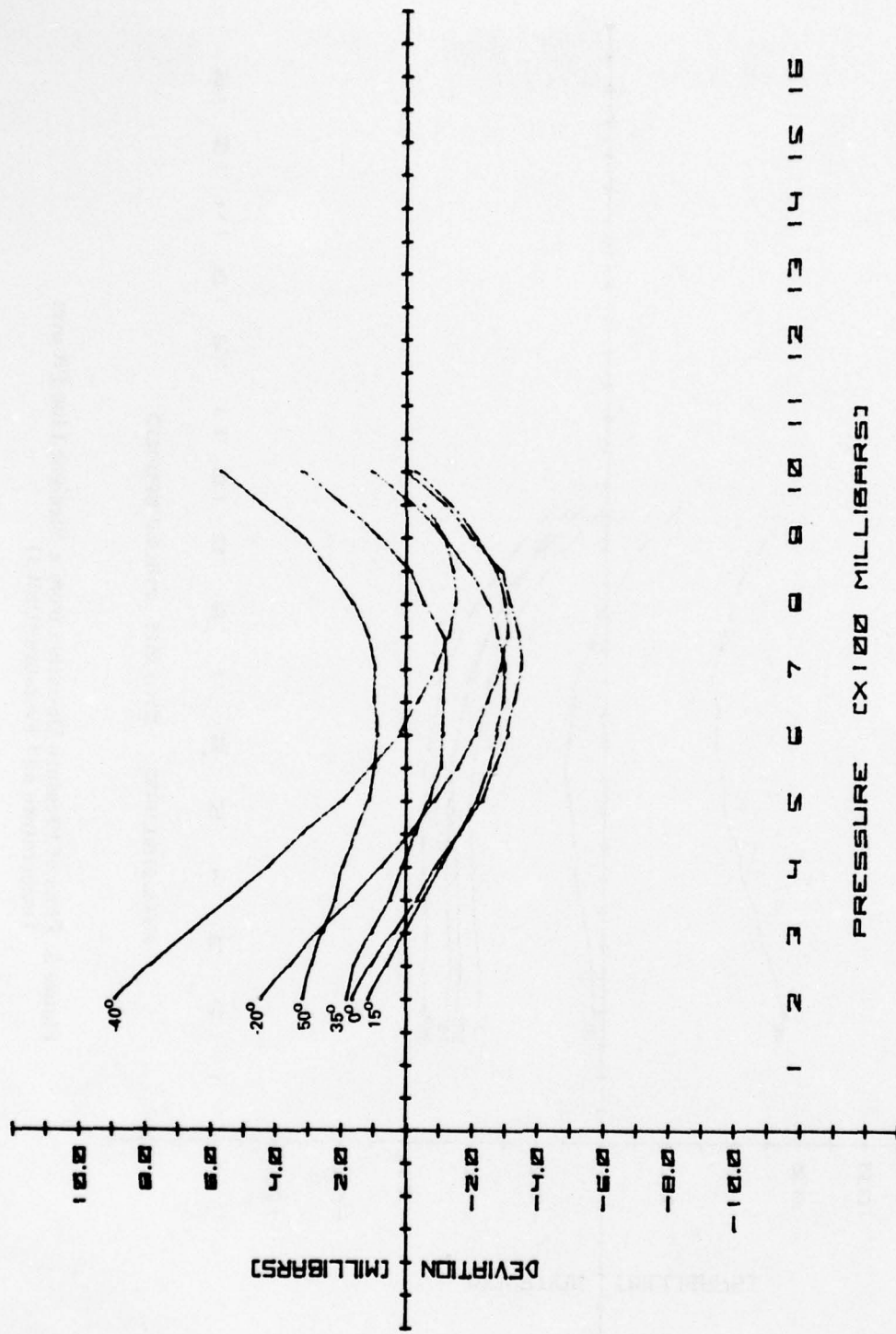


Figure 6. Plots of Pressure Deviation from a Straight Line Fit over Temperature and Pressure (Unit 2)

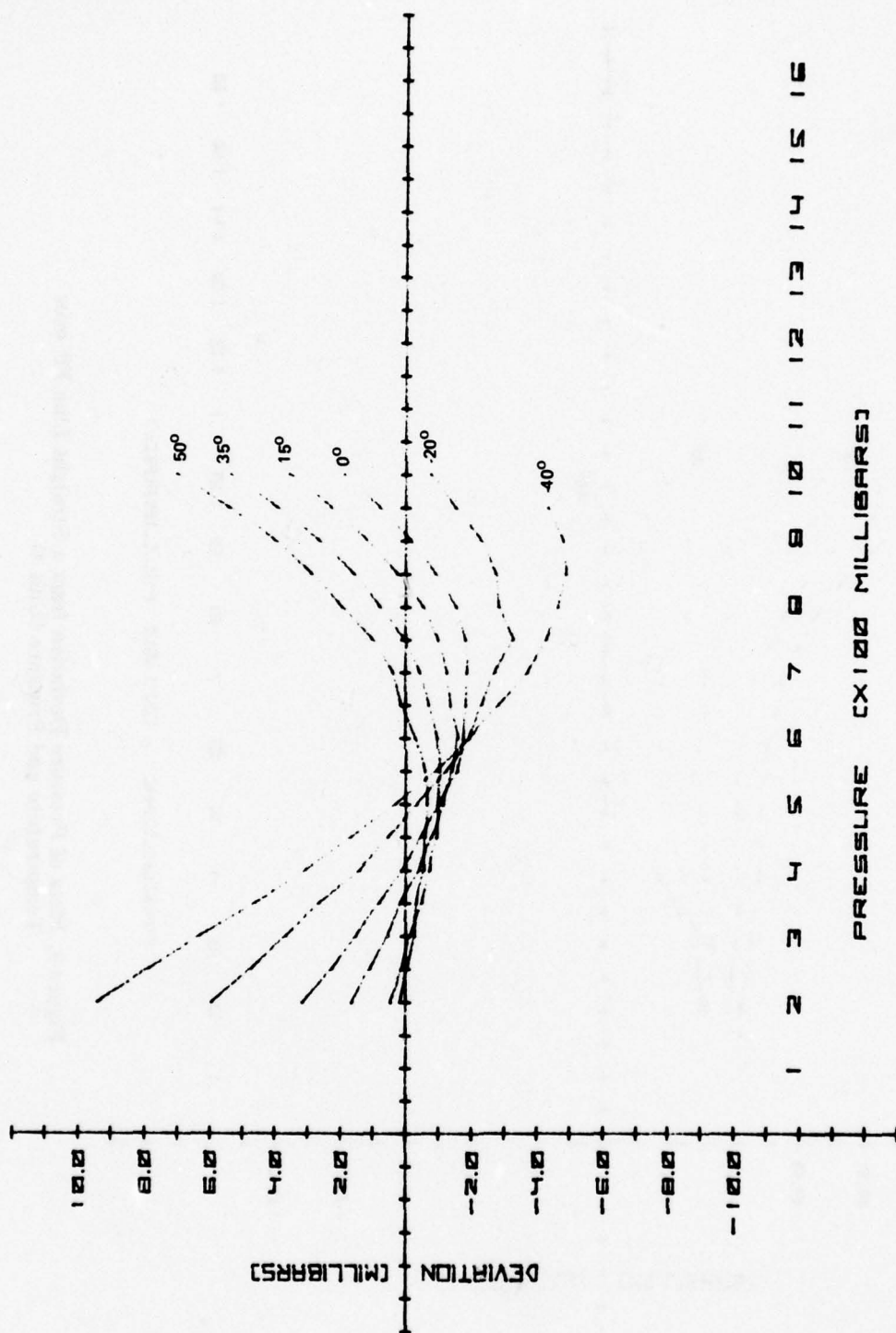


Figure 7. Plots of Pressure Deviation from a Straight Line Fit over Temperature and Pressure (Unit 3)

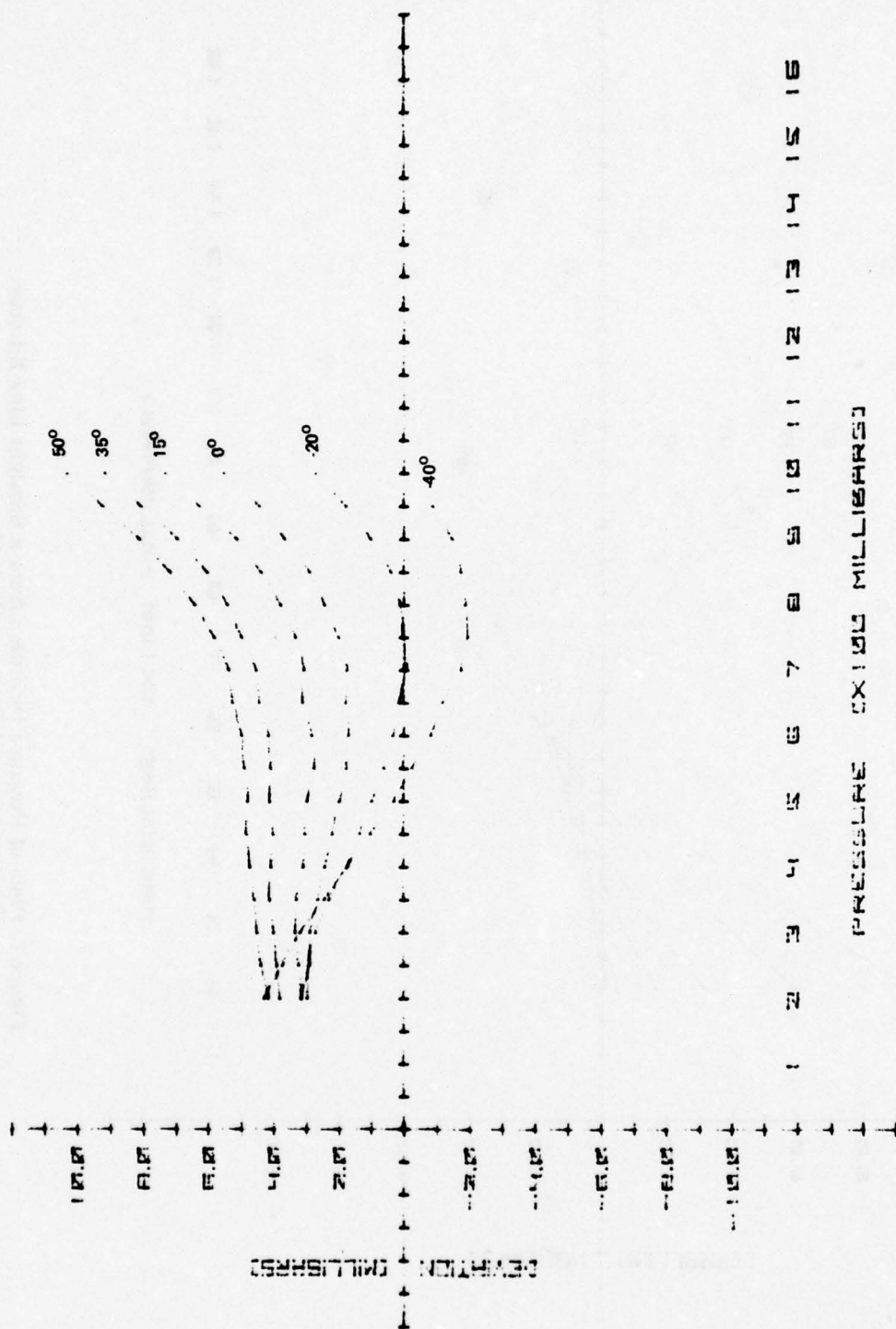


Figure 8. Plots of Pressure Deviation from a Straight Line Fit over Temperature and Pressure (Unit 4)

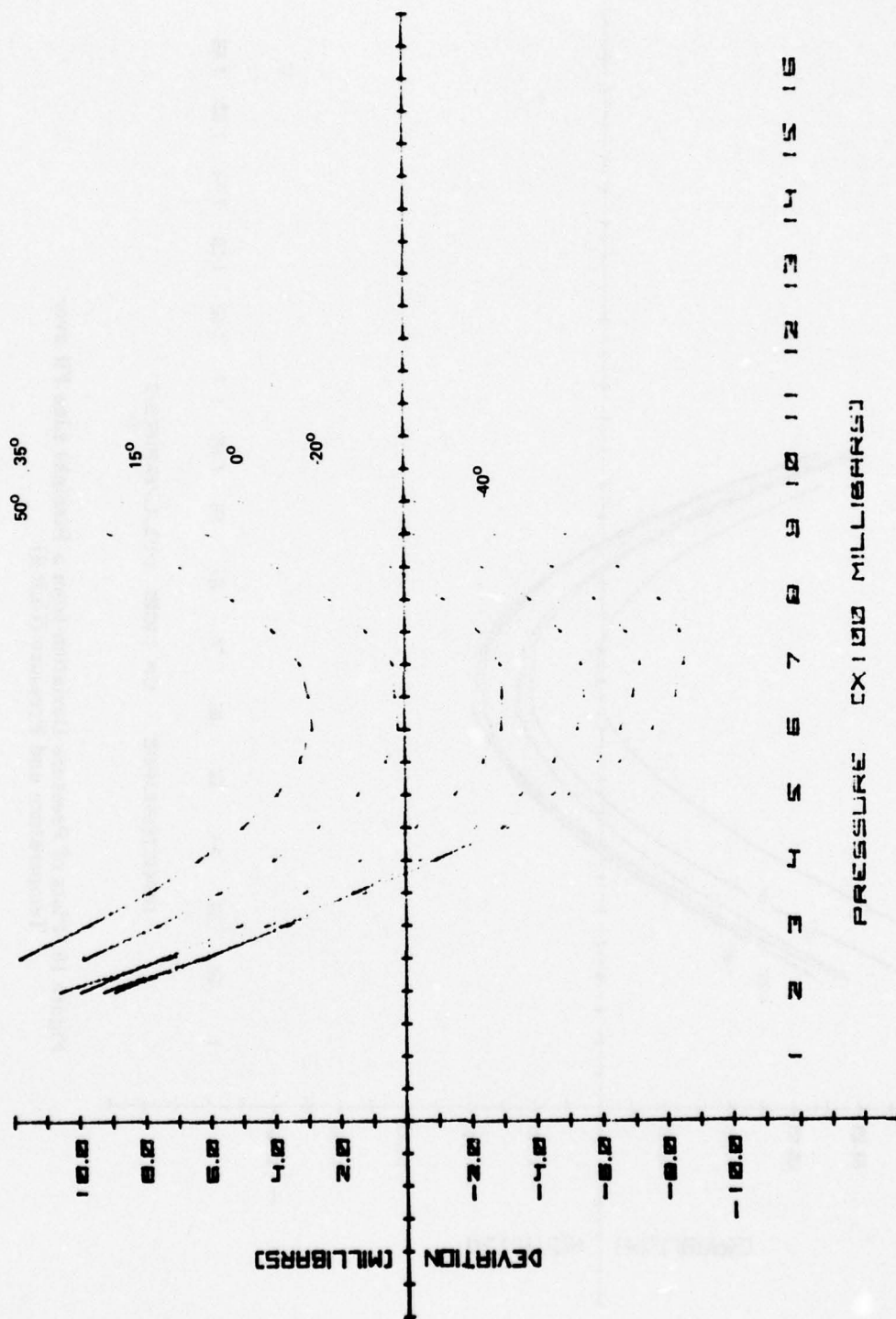


Figure 9. Plots of Pressure Deviation from a Straight Line Fit over Temperature and Pressure (Unit 5)

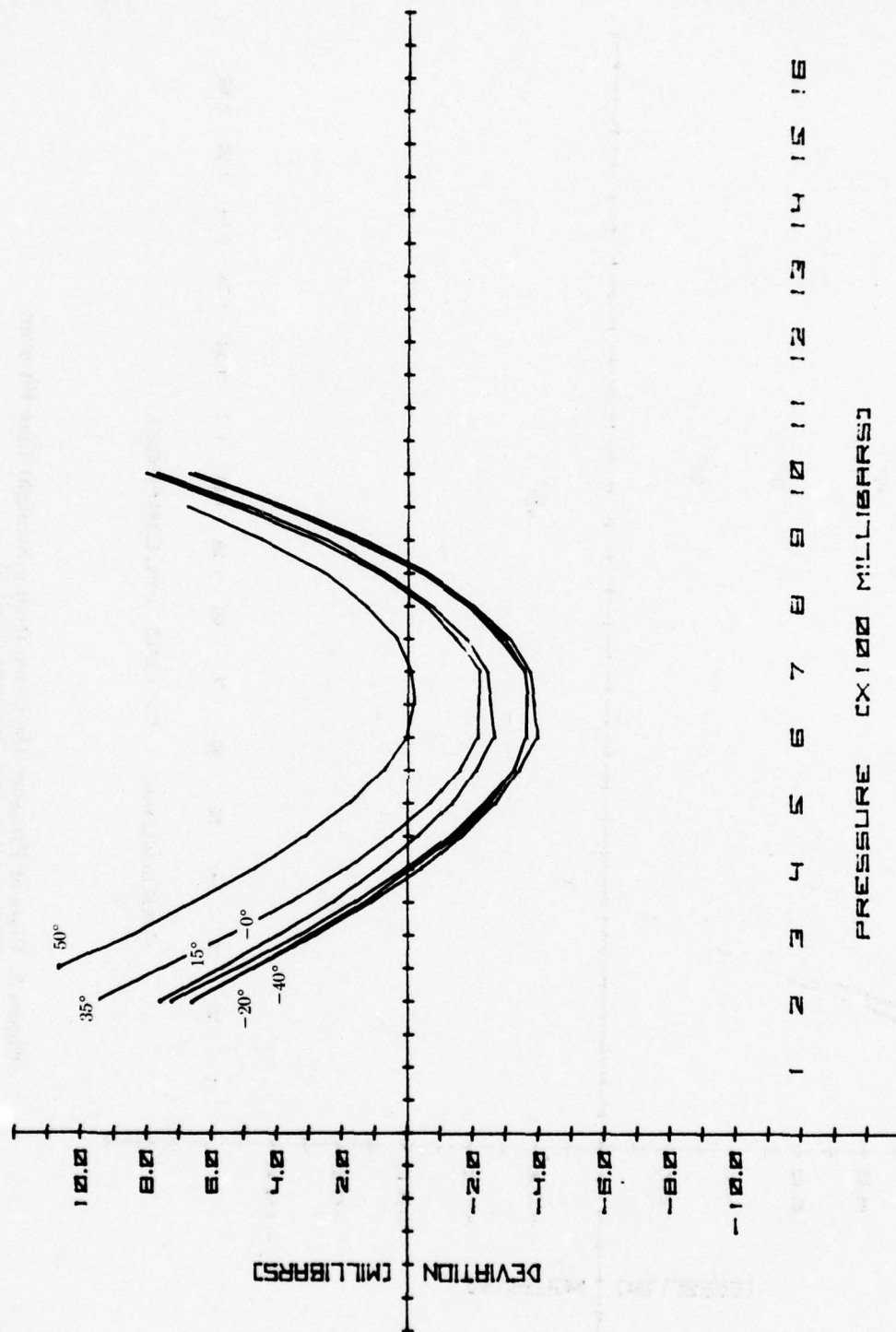


Figure 10. Plots of Pressure Deviation from a Straight Line Fit over Temperature and Pressure (Unit 6)

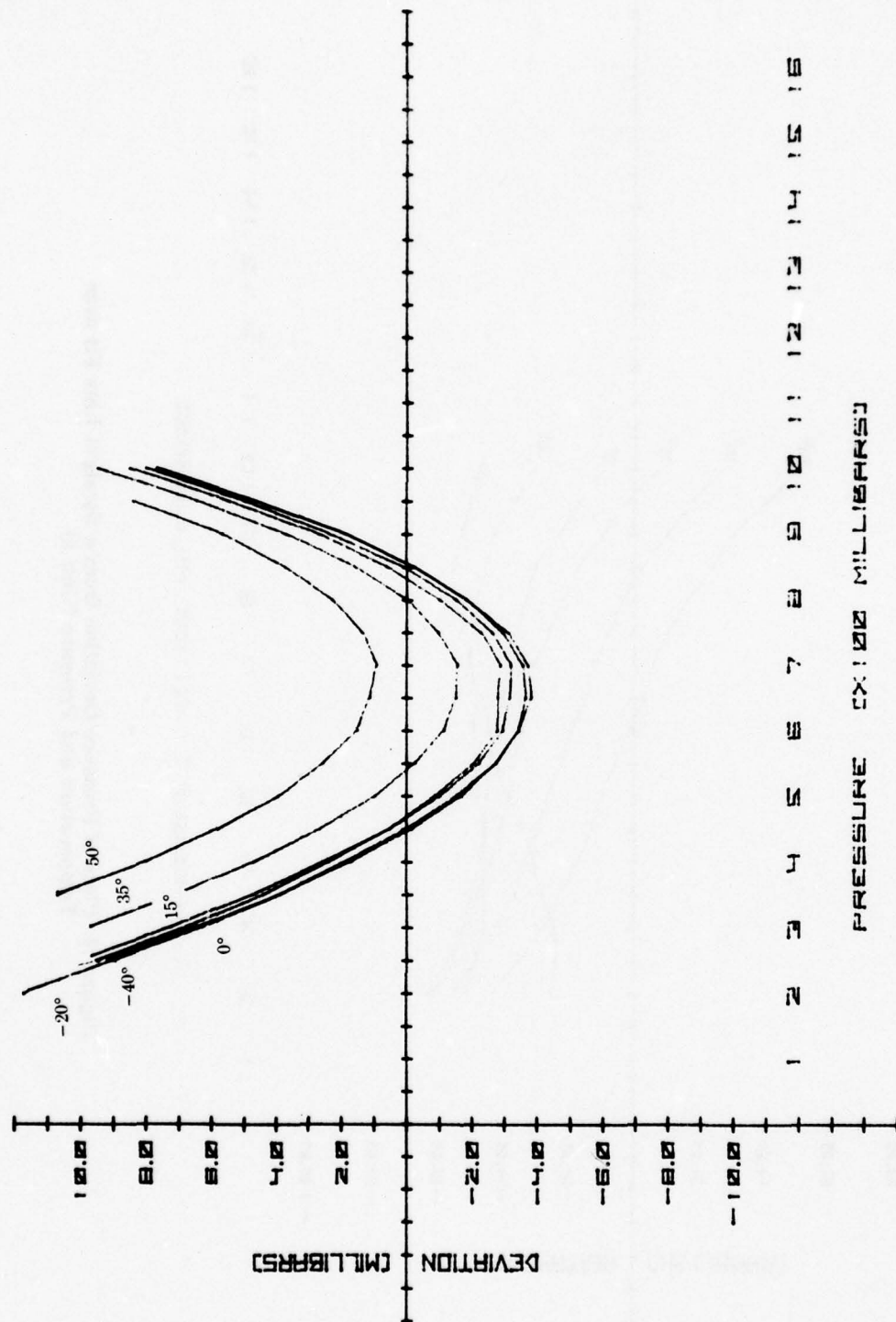


Figure 11. Plots of Pressure Deviation from a Straight Line Fit over Temperature and Pressure (Unit 7)

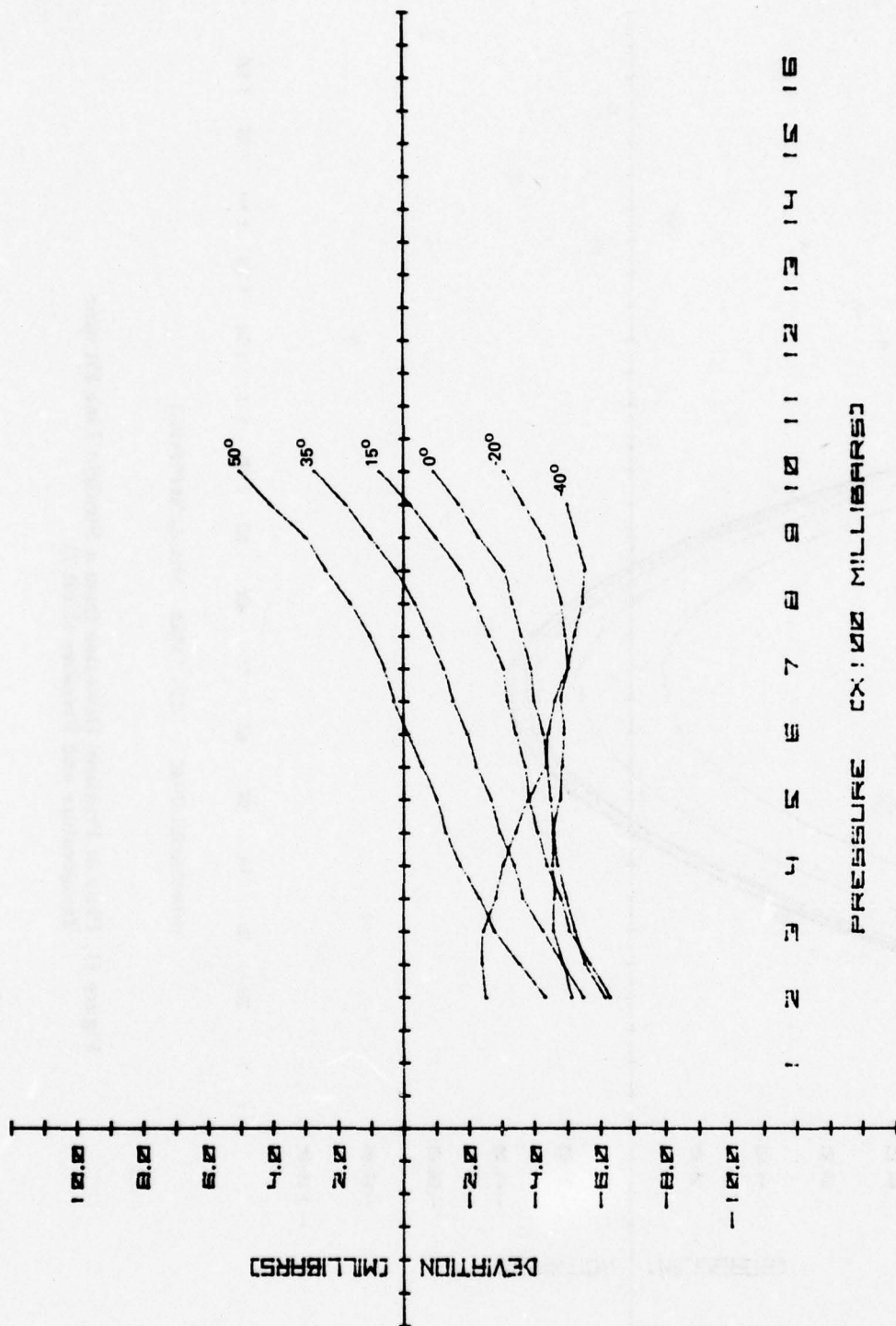


Figure 12. Plots of Pressure Deviation from a Straight Line Fit over Temperature and Pressure (Unit 8)

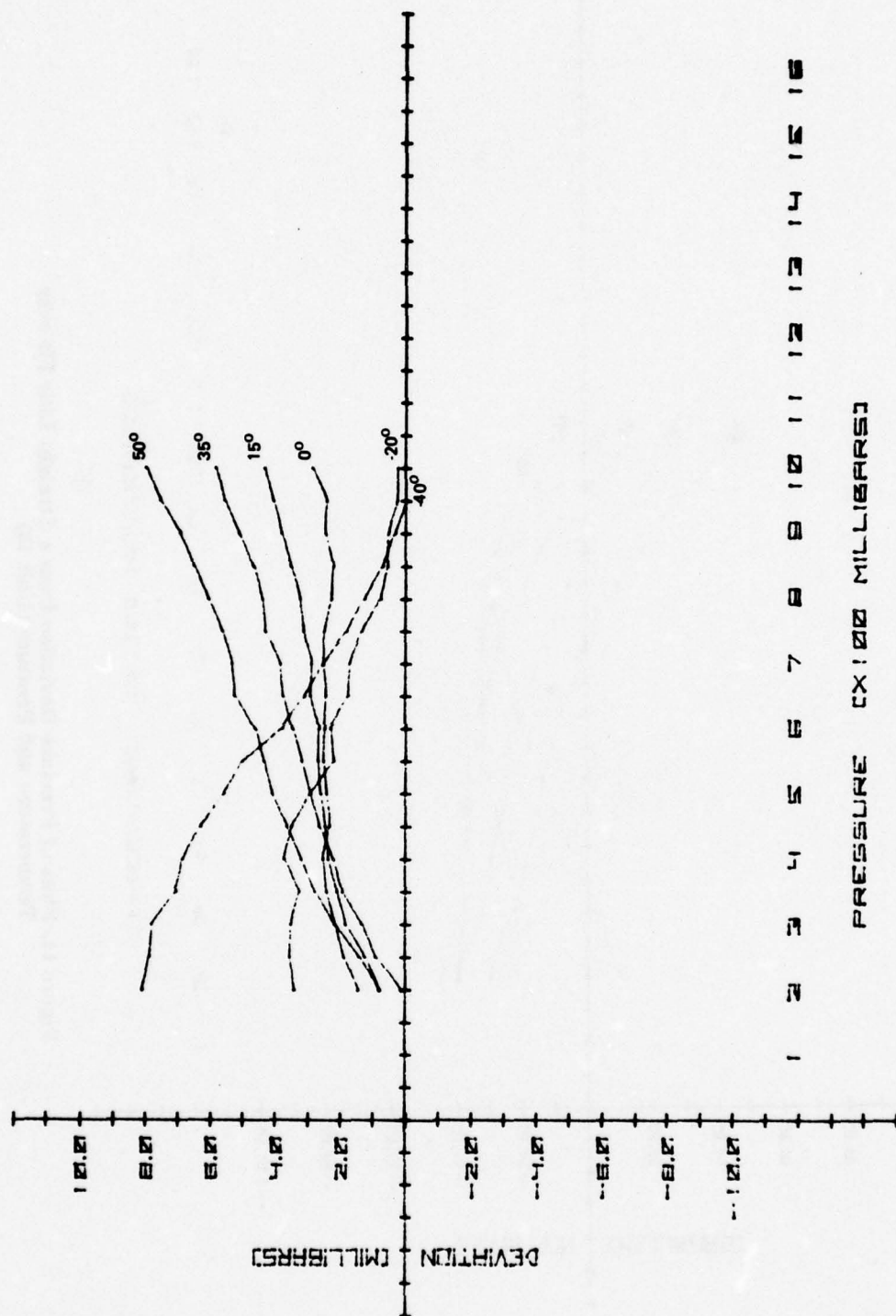


Figure 13. Plots of Pressure Deviation from a Straight Line Fit over Temperature and Pressure (Unit 9)

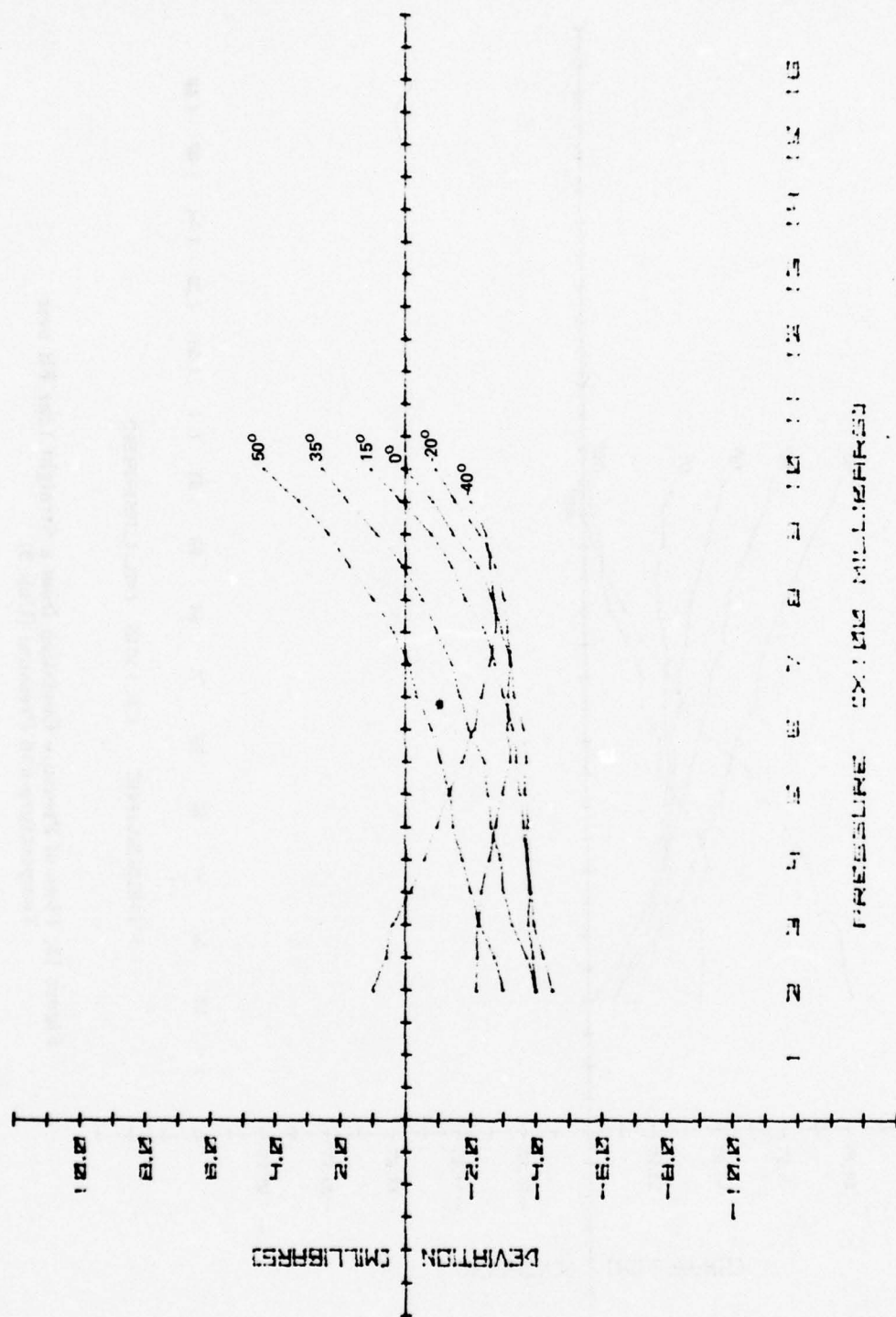


Figure 14. Plots of Pressure Deviation from a Straight Line Fit over Temperature and Pressure (Unit 10)

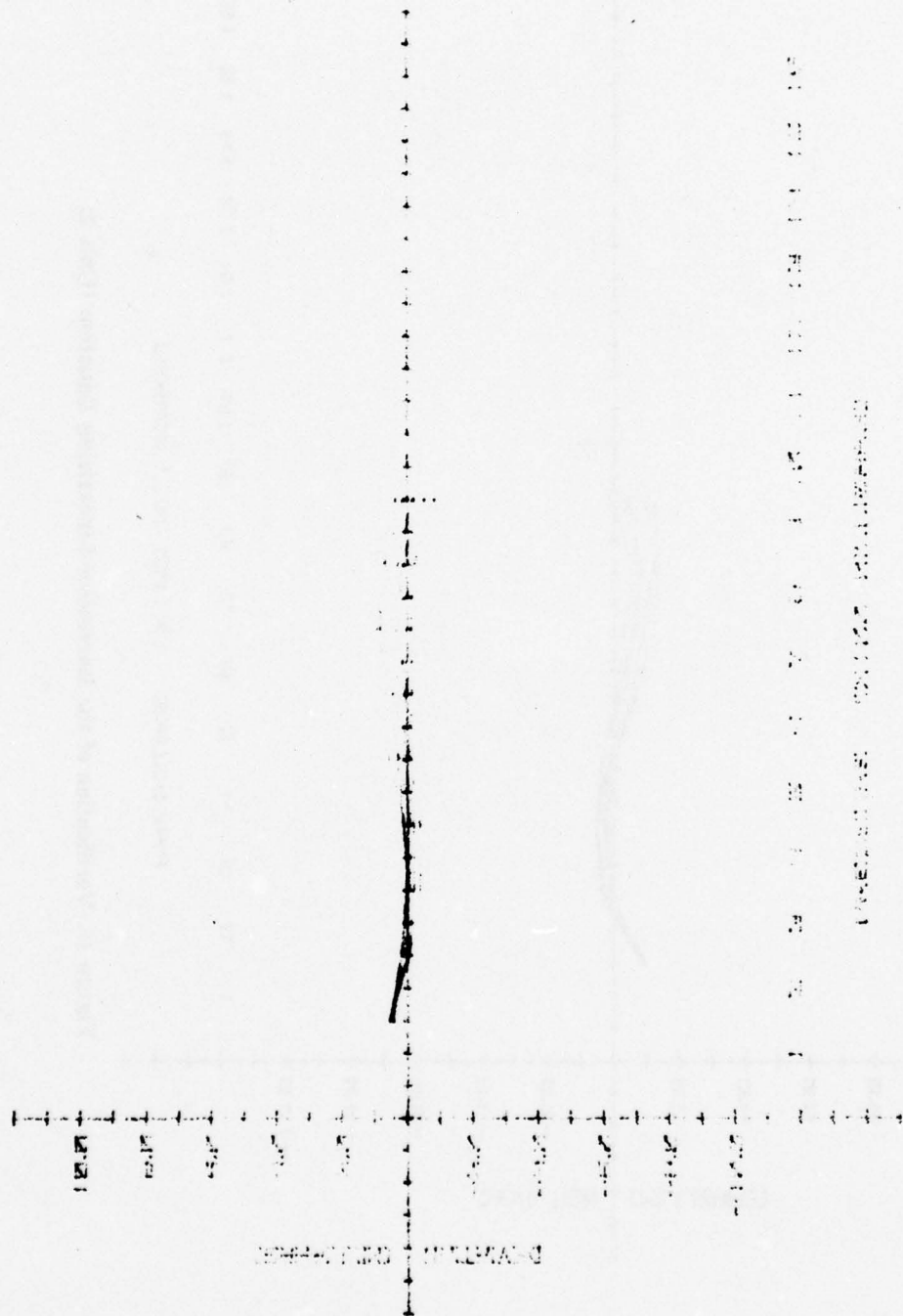


Figure 15. Verification of the Barometer Linearizing Equation (Unit 1)

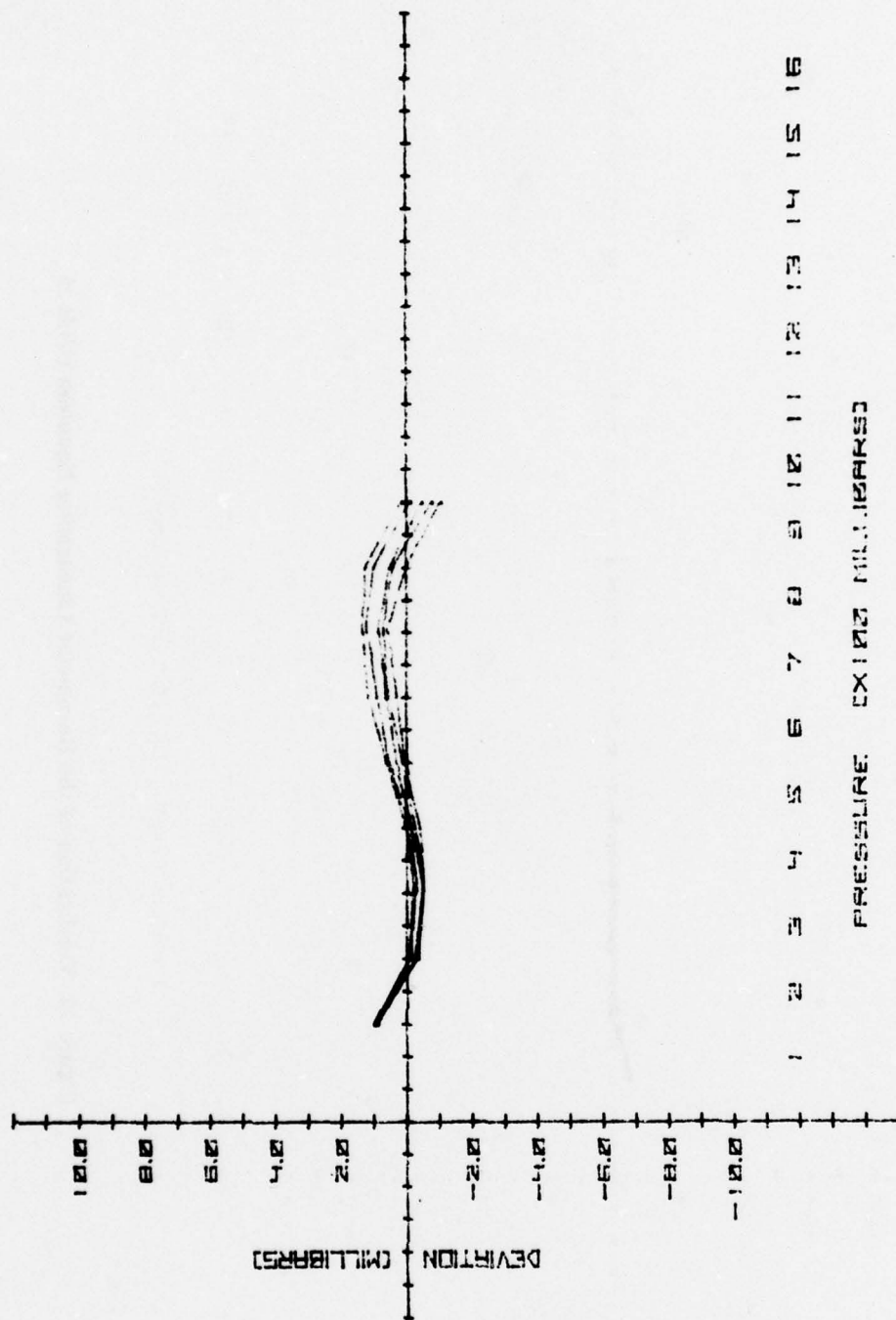


Figure 16. Verification of the Barometer Linearizing Equation (Unit 2)

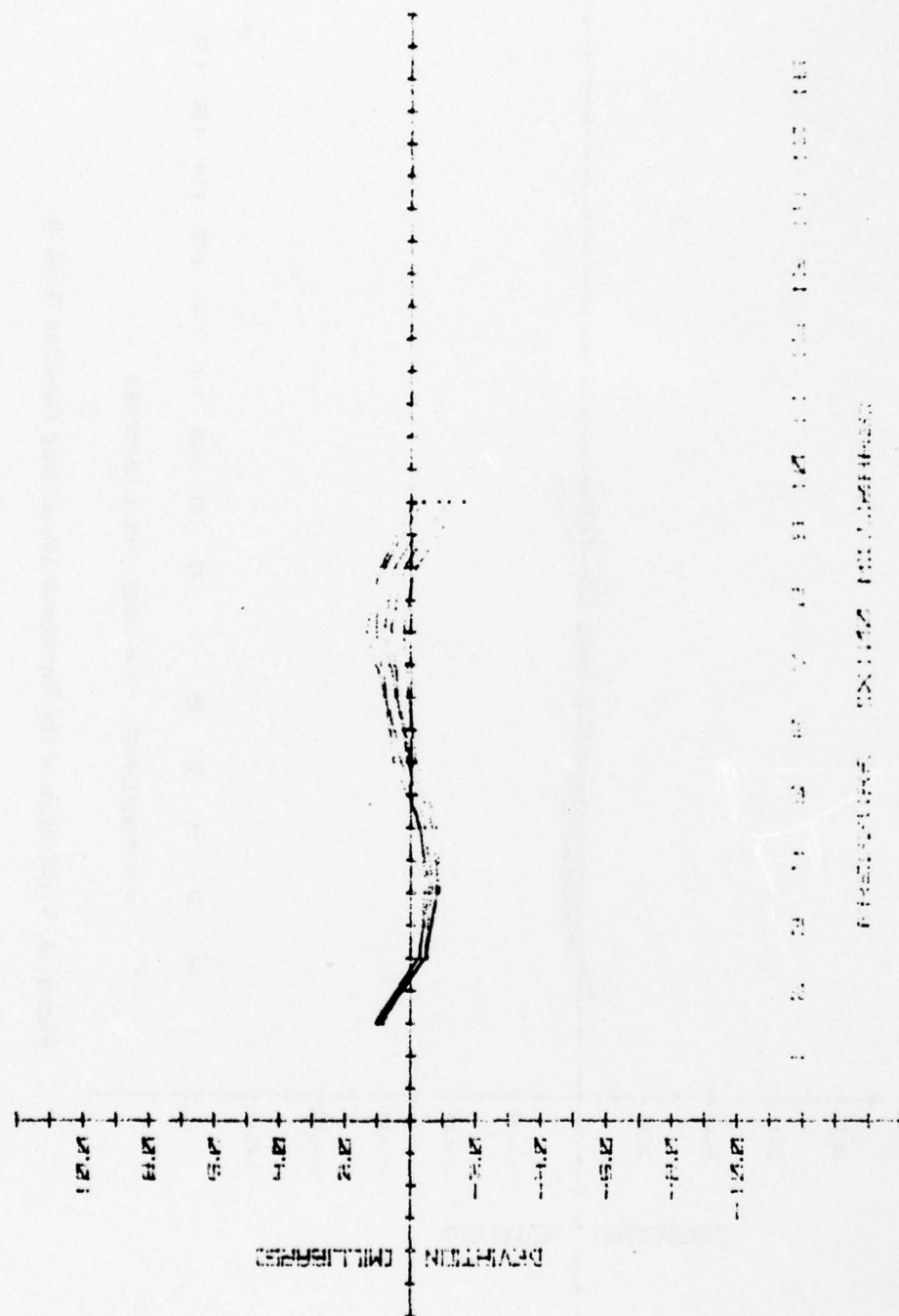


Figure 17. Verification of the Barometer Linearizing Equation (Unit 3)

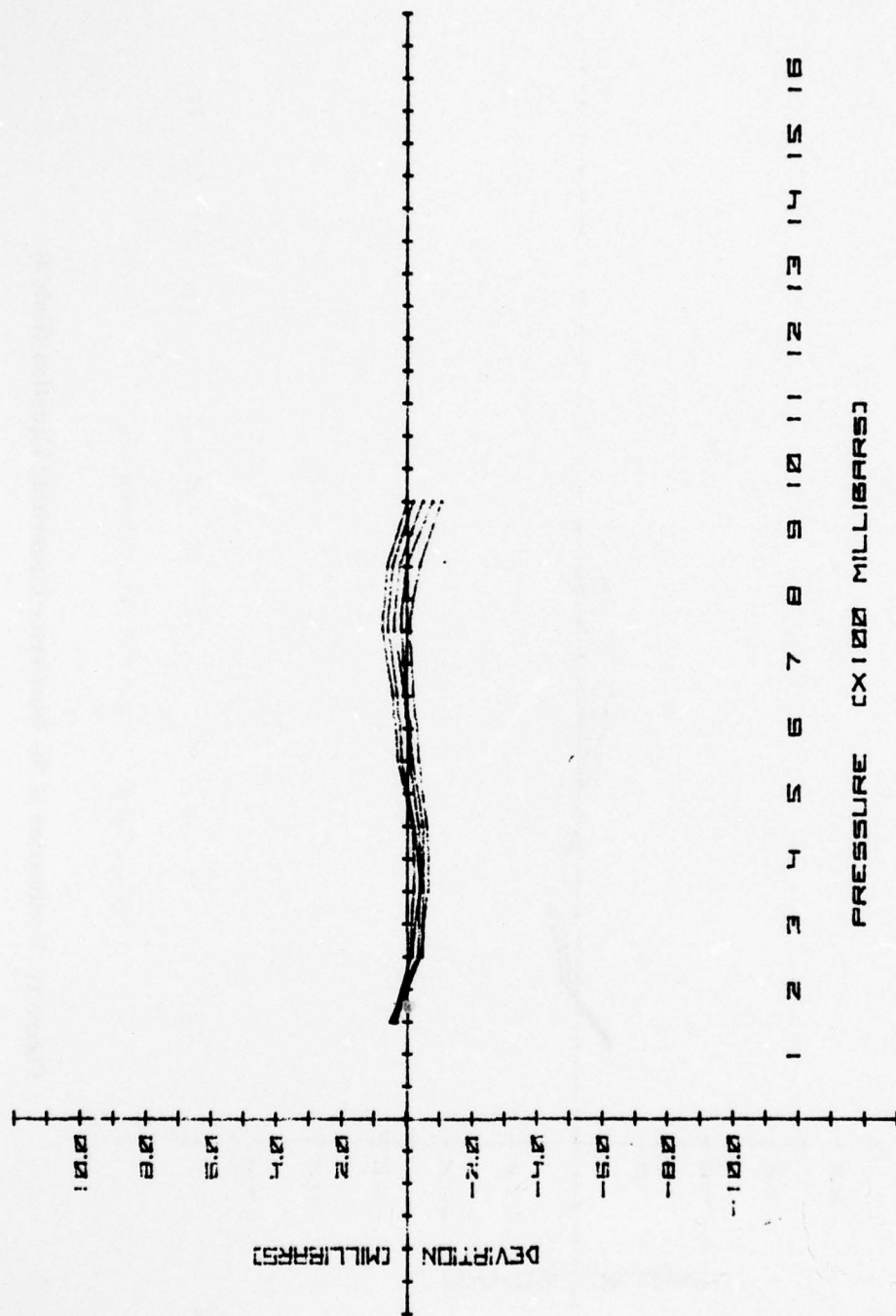


Figure 18. Verification of the Barometer Linearizing Equation (Unit 4)

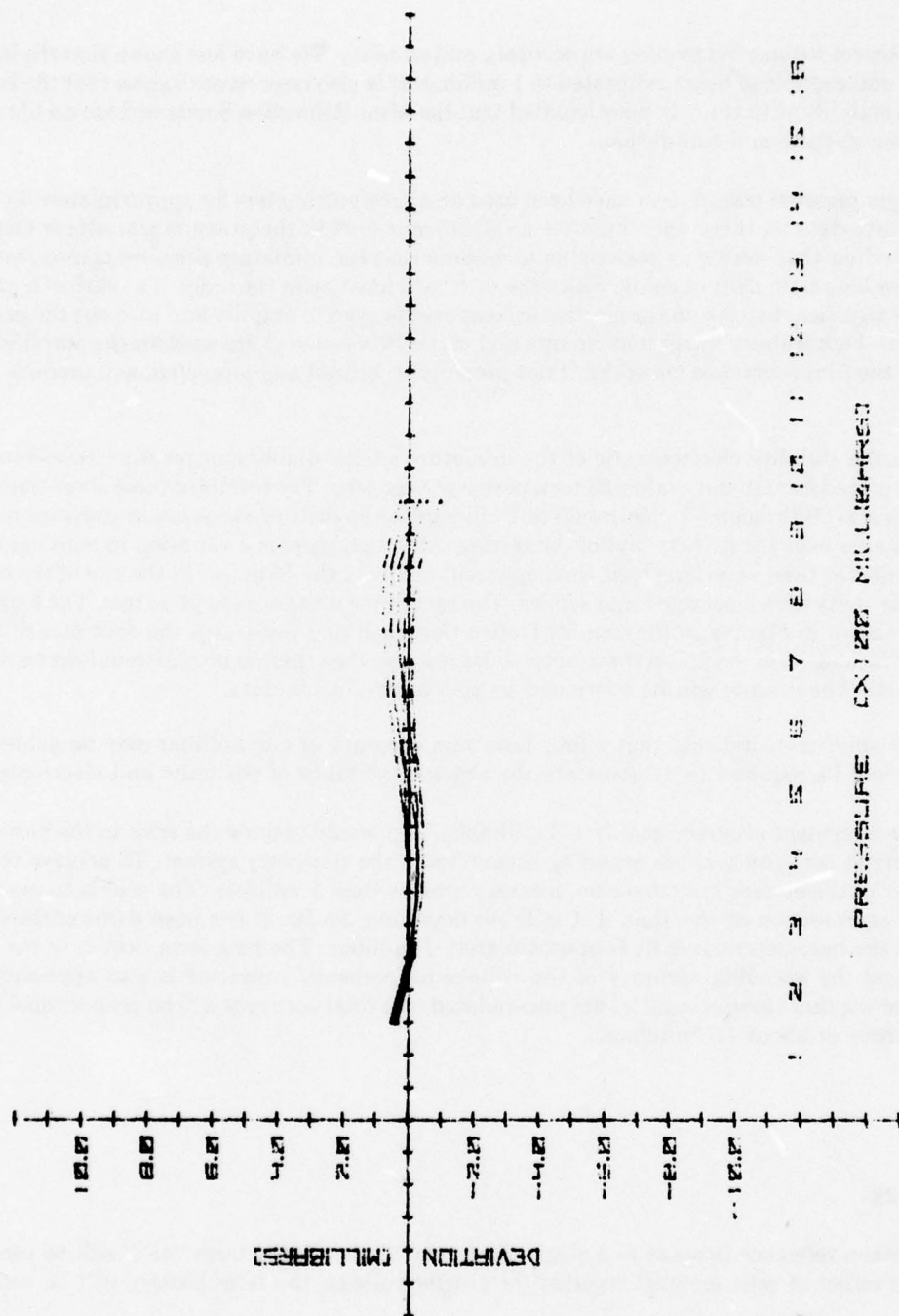


Figure 19. Verification of the Barometer Linearizing Equation (Unit 5)

2. Stability

Two parts of a correct barometric reading are accuracy and stability. We have just shown that the barometer is accurate and capable of being calibrated to 1 millibar. It is also important to show that the barometer retains this stability with time. It is anticipated that the Mini-Refracton Sonde will have a life of 2 to 5 years after manufacture and calibration.

Silicon diaphragm pressure transducers have been used on aircraft altimeters for approximately 10 years. Long term stability data on these units indicate no significant drift in the pressure transducer elements themselves. Based on that data it is reasonable to assume that the miniature pressure transducers will also exhibit a low long term drift or aging. Since the drift rate must be in the order of a tenth of a percent or less, this puts significant strain on the electronic components used to amplify and read out the pressure signal. In general, high stability integrated circuits and metal film resistors are used for the amplifier networks. Some of the film resistance networks, if not properly stabilized and protected, will produce unacceptable drift.

To demonstrate the stability characteristic of the miniature silicon diaphragm pressure transducer, 10 units have been placed on test and evaluated for a period of 8 months. The results of these short term tests are shown in Figures 20 through 35. Figures 20 to 25 illustrate the drift or variation in pressure reading for all 10 transducers over the first 80 days of the testing. Although there is a variation in readings of approximately a millibar there is no long term drift apparent in any of the 10 units. At the end of the 80-day period, five of the units were assembled into sondes. The remaining units were kept on test. The long term test results are shown in Figures 26 through 35. Notice that each plot illustrates the drift at a different pressure level. The long term results on these units illustrate also that there is no apparent long term drift trend in the units. These units will be continued on test to obtain life data.

These relatively short tests indicate that a long term rms accuracy of one millibar may be achievable. Further testing will be required to demonstrate the absolute stability of the units and electronics.

The pressure measurement accuracy goal is ± 3 millibars. This would include the error in the barometer accuracy, barometer stability and the encoding accuracies of the telemetry system. To achieve this accuracy each part of the system must have an accuracy greater than 1 millibar. The goal is to maintain the accuracy of each section at less than ± 1 millibar deviation. So far, it has been demonstrated that the accuracy of the barometer curve fit is approximately 1 millibar. The long term drift is in the order of 1 millibar, and the encoding accuracy of the voltage-to-frequency converter is also approximately 1 millibar. Assuming that these accuracies are uncorrelated, the total accuracy will be proportional to the square root of three or about 1.7 millibars.

B. BATTERY

1. Requirements

In this report, when reference is made to a single electrochemical cell, the term "cell" will be used. For reference to a number of cells grouped together for greater voltage, the term battery will be used.

There are several conflicting requirements for the minisonde battery. The battery must be very lightweight, capable of providing a high current drain and have a good shelf life so that it can be installed in the sonde at the time of manufacture. A goal of less than 30 grams per battery is desirable.

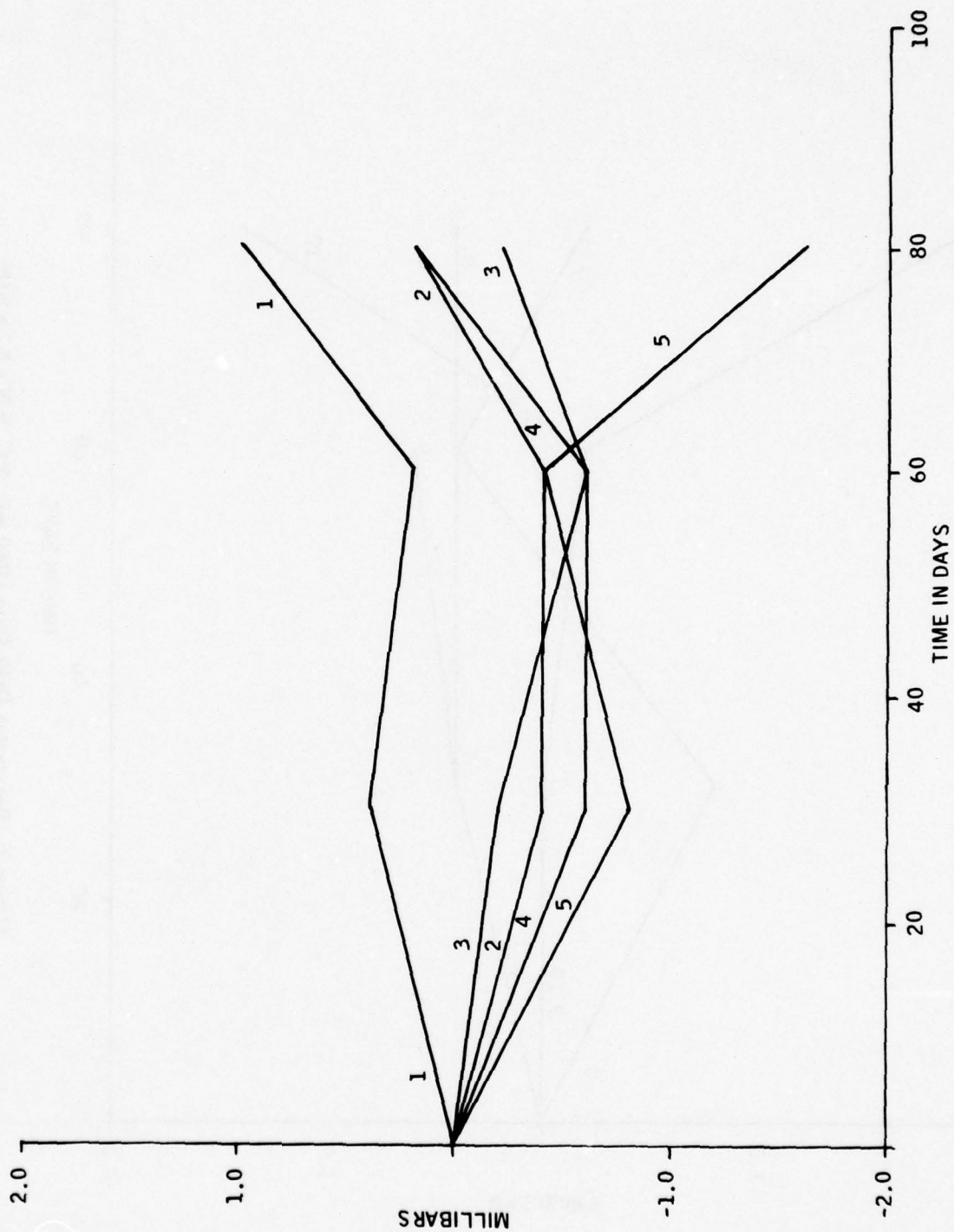


Figure 20. Barometer Drift Data (1000 mB, 0°C, S/N's 1,2,3,4,5)

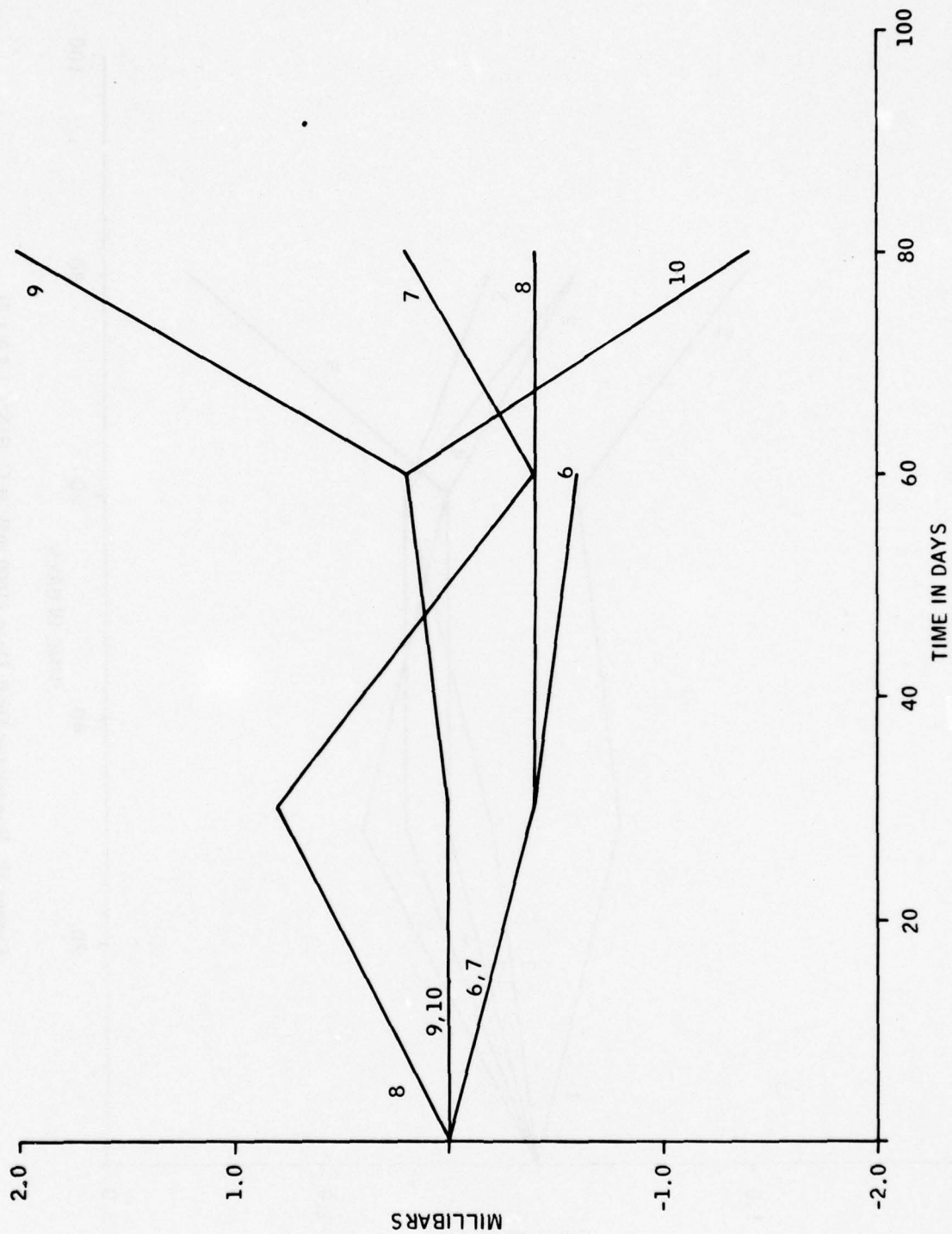


Figure 21. Barometer Drift Data (1000 mB, 0°C, S/N's 6,7,8,9,10)



Figure 22. Barometer Drift Data (600 mB, 0°C, S/N's 1,2,3,4,5)

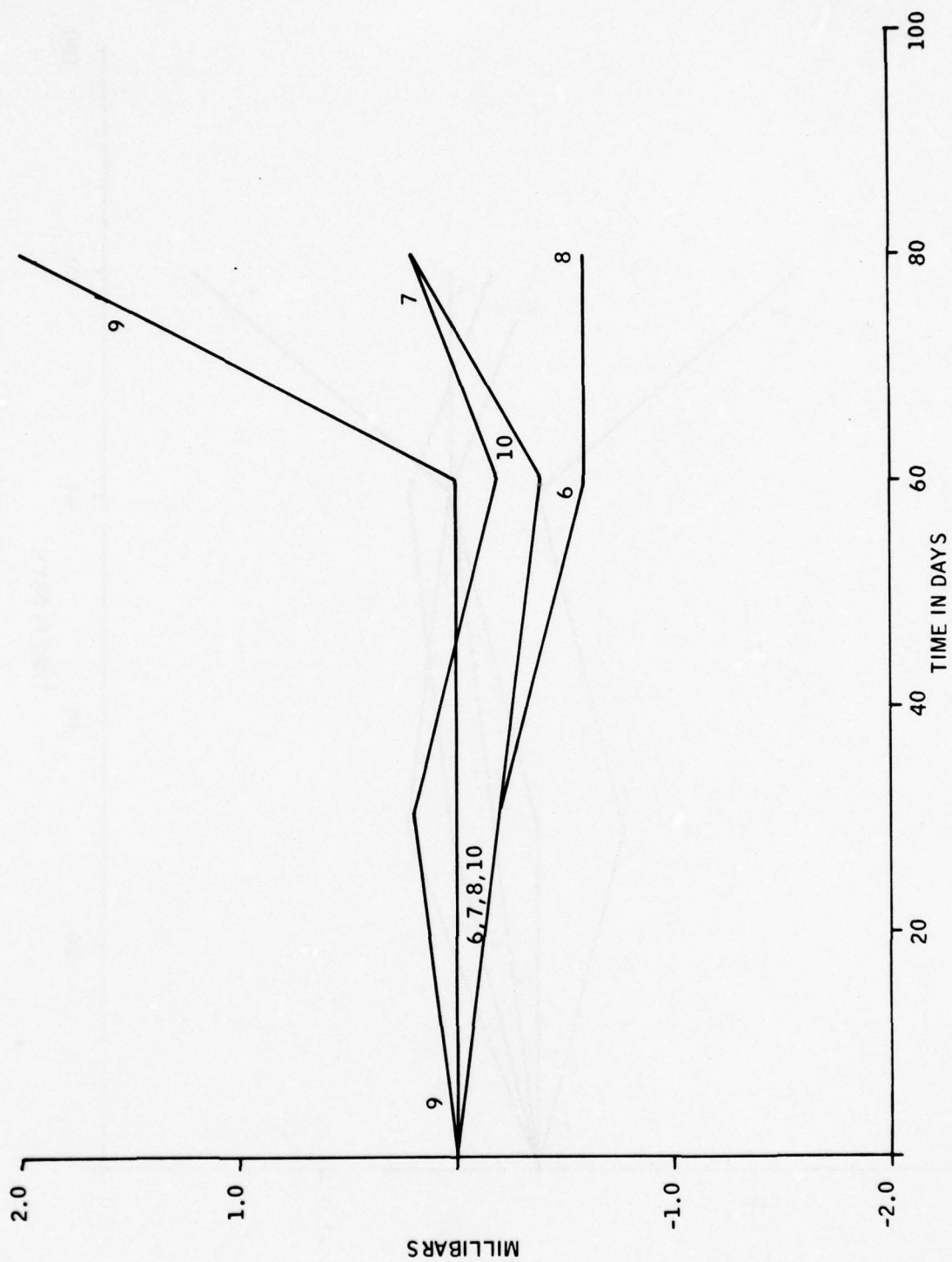


Figure 23. Barometer Drift Data (600 mB, 0°C, S/N's 6,7,8,9,10)

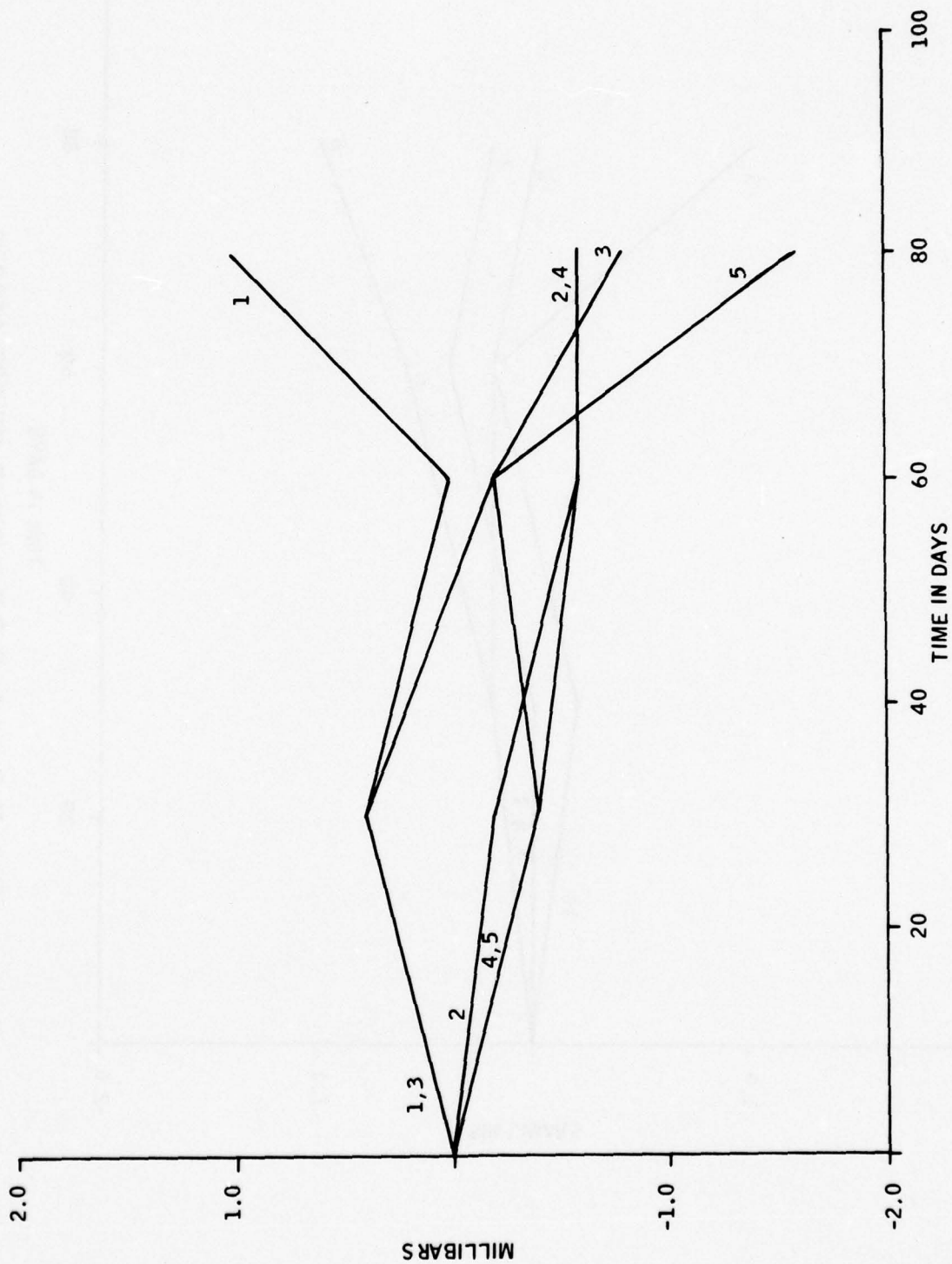


Figure 24. Barometer Drift Data (200 mB, 0°C, S/N's 1,2,3,4,5)

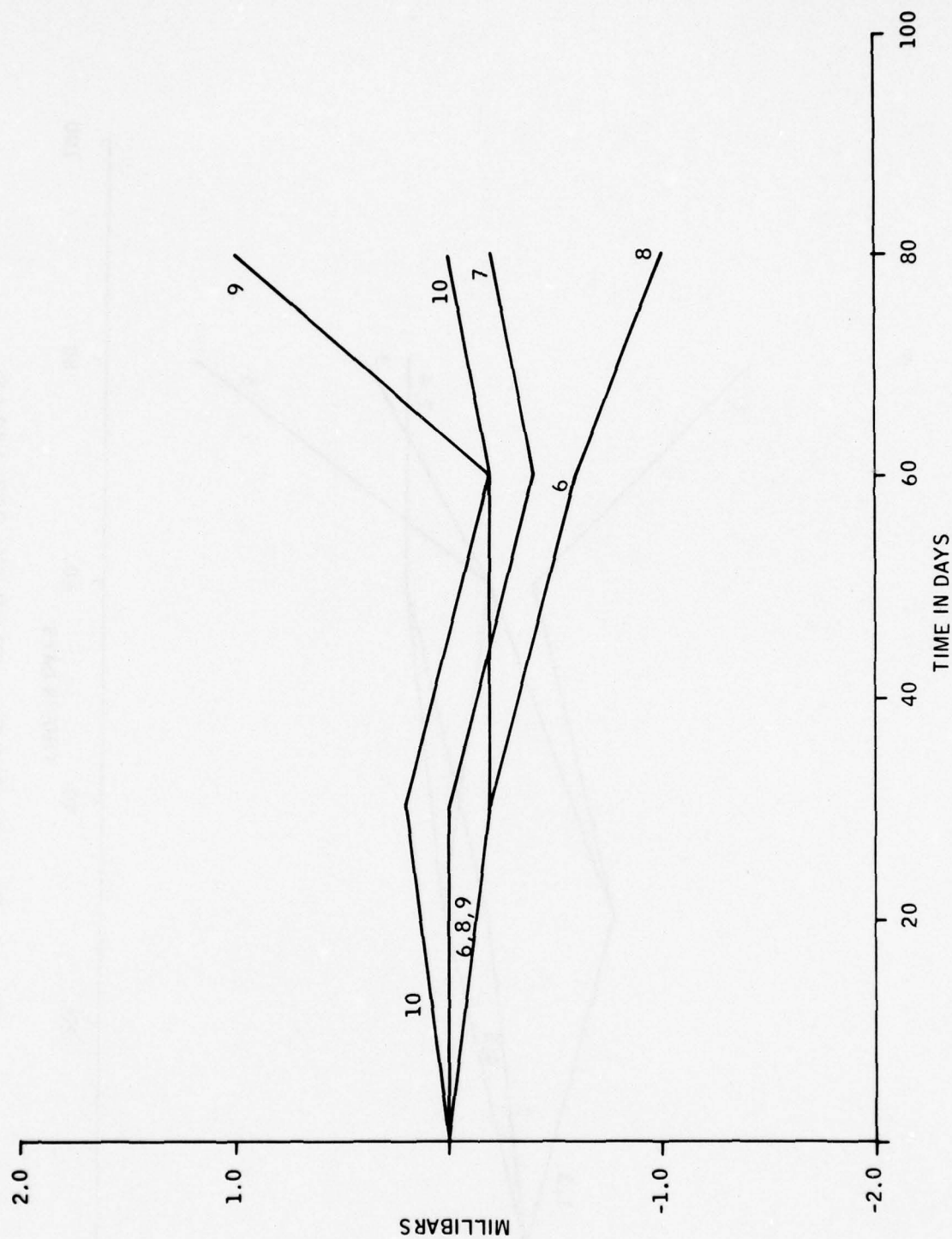


Figure 25. Barometer Drift Data (200 mB, 0°C, S/N's 6,7,8,9,10)

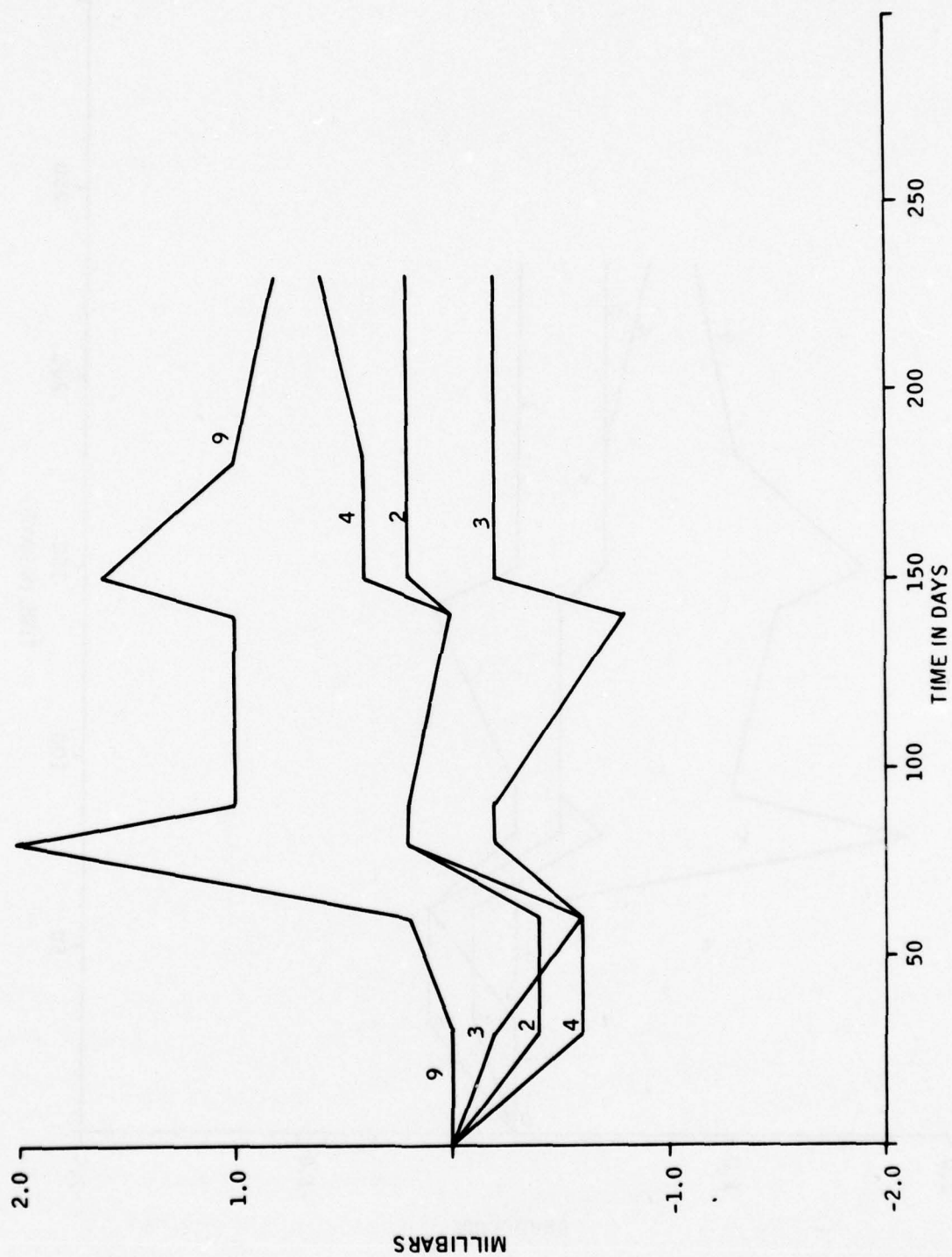


Figure 26. Barometer Drift Data (1000 mB, 0°C)



Figure 27. Barometer Drift Data (900 mB, 0°C)

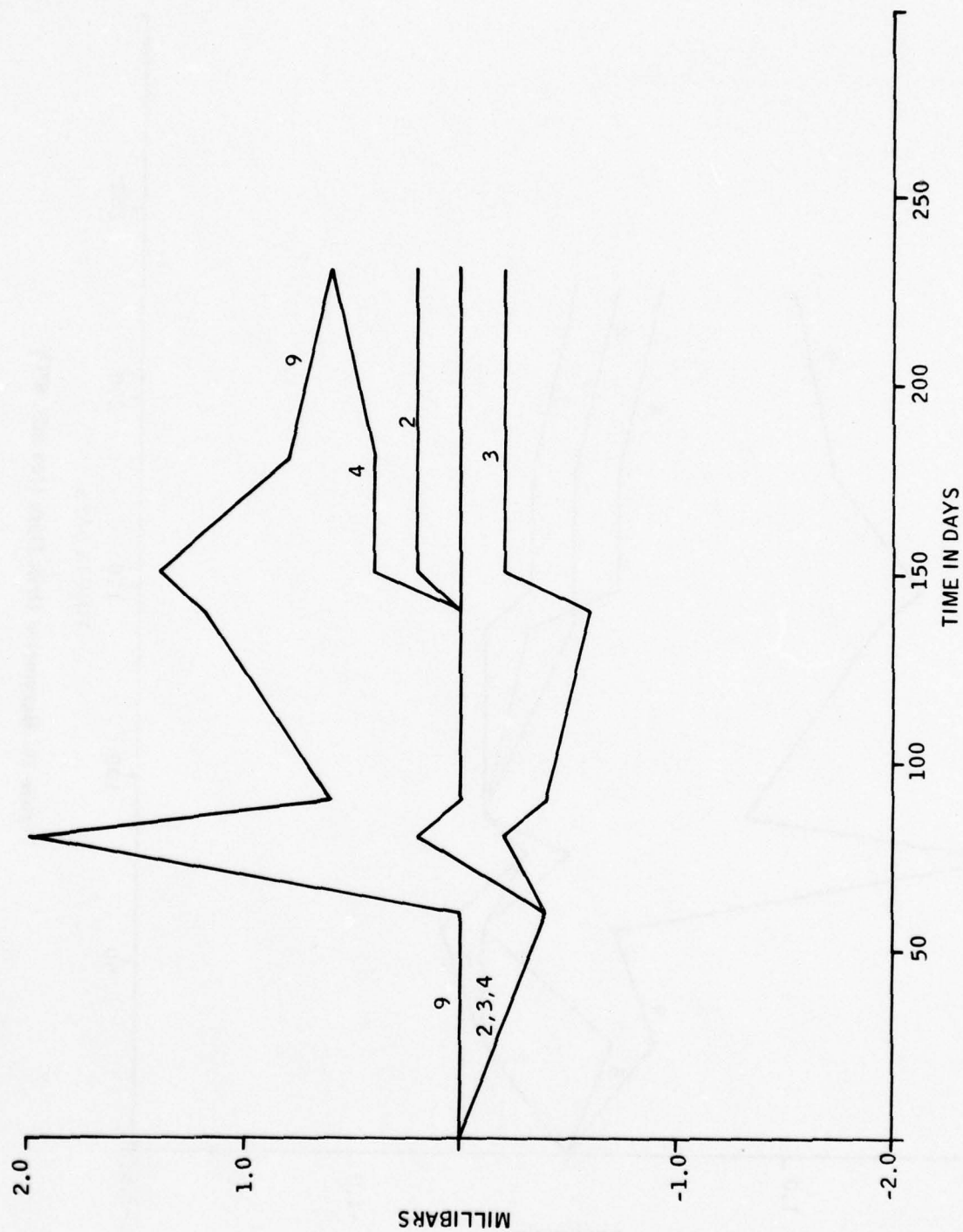


Figure 28. Barometer Drift Data (800 mB, 0°C)

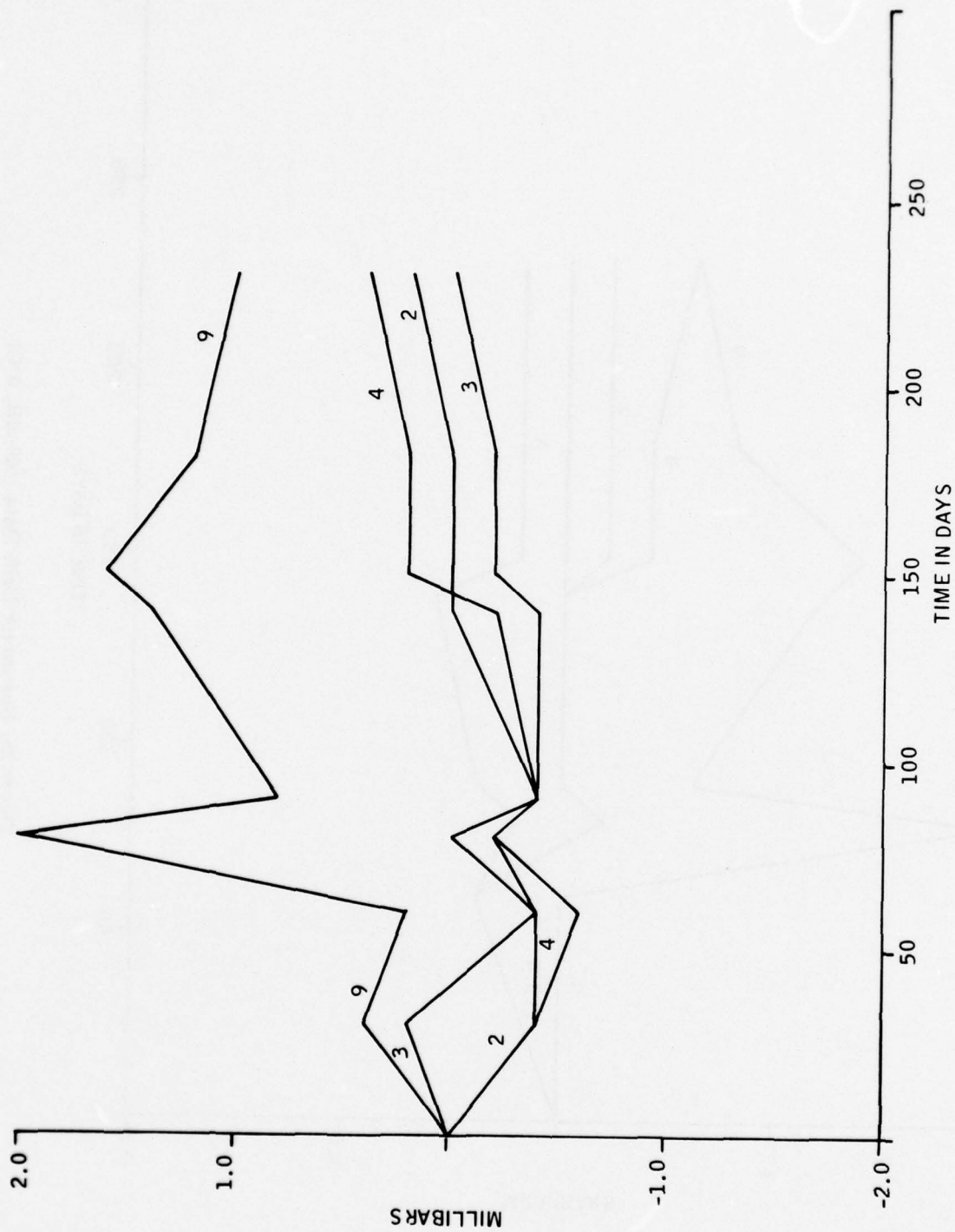


Figure 29. Barometer Drift Data (700 mB, 0°C)

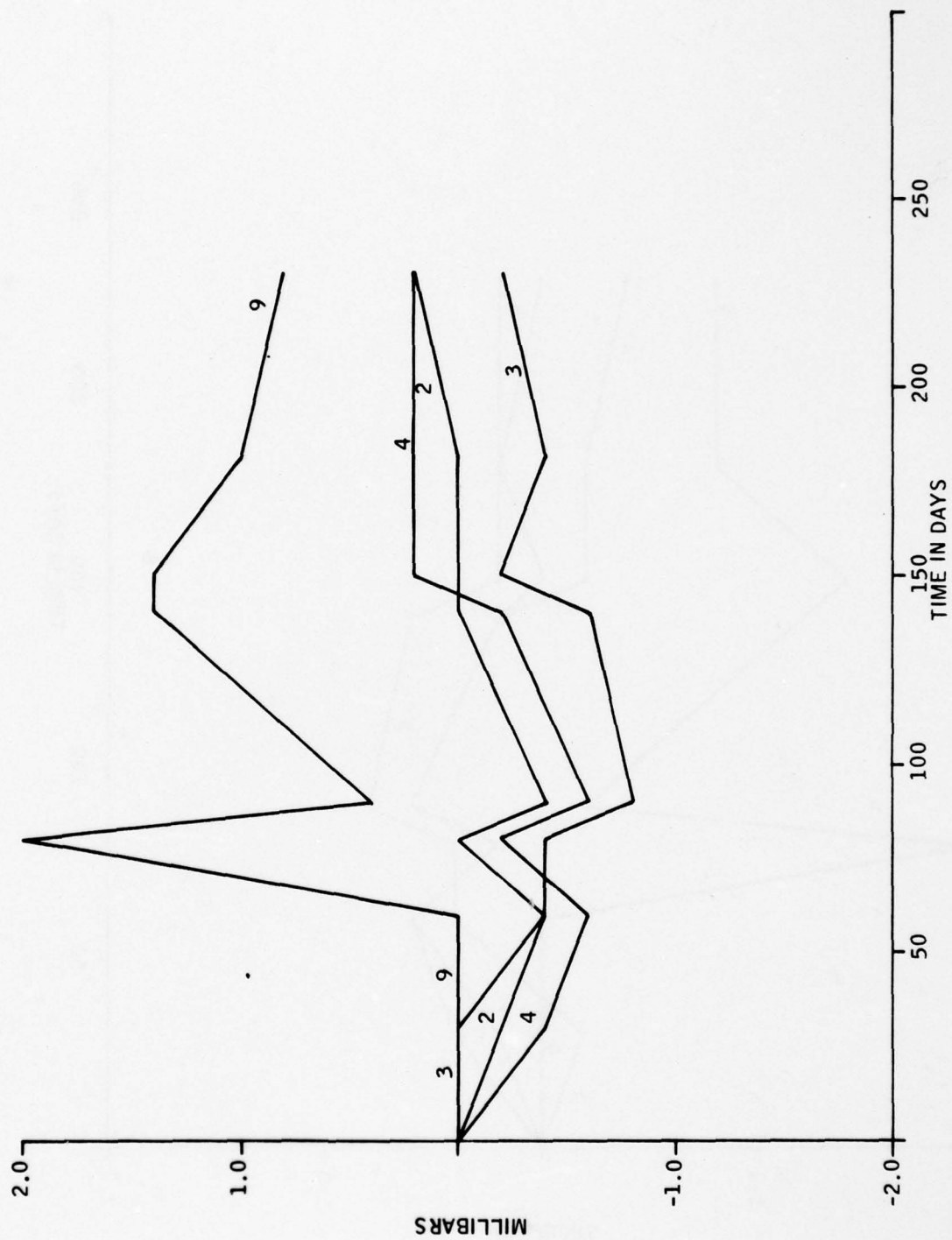


Figure 30. Barometer Drift Data (600 mB, 0°C)



Figure 31. Barometer Drift Data (500 mB, 0°C, S/N's 2,3,4,9)

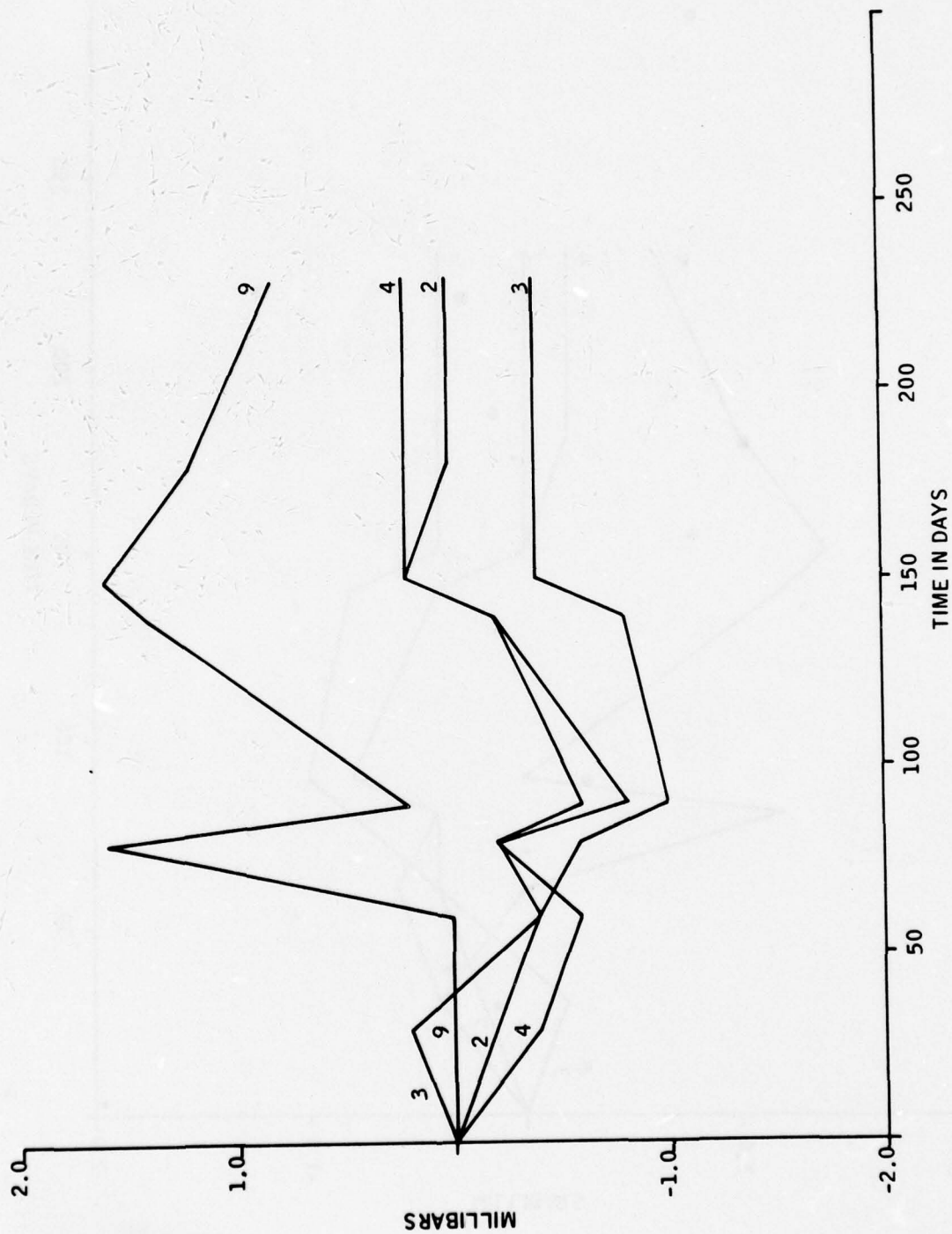


Figure 32. Barometer Drift Data (400 mB, 0°C, S/N's 2,3,4,9)

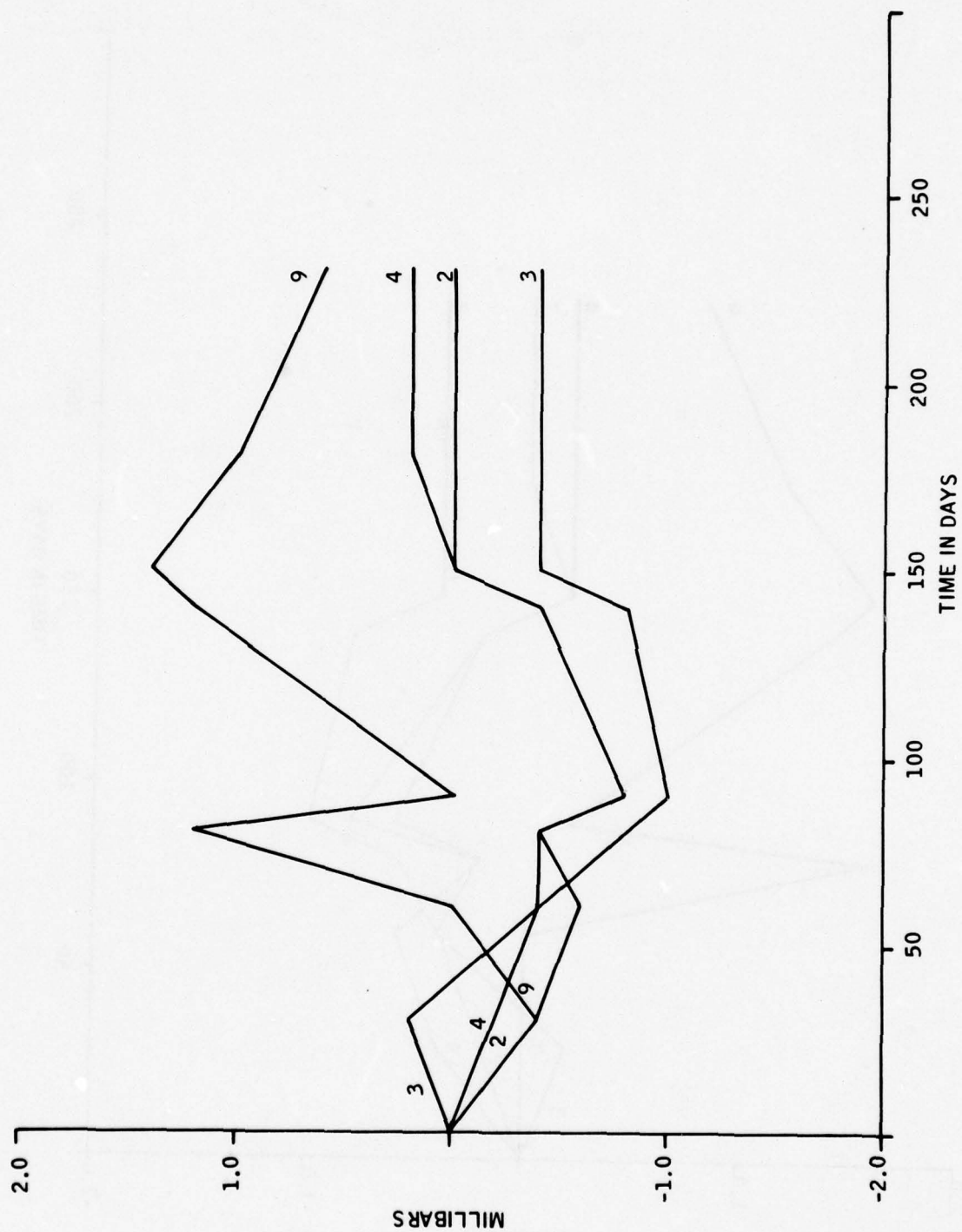


Figure 33. Barometer Drift Data (300 mB, 0°C, S/N's 2,3,4,9)

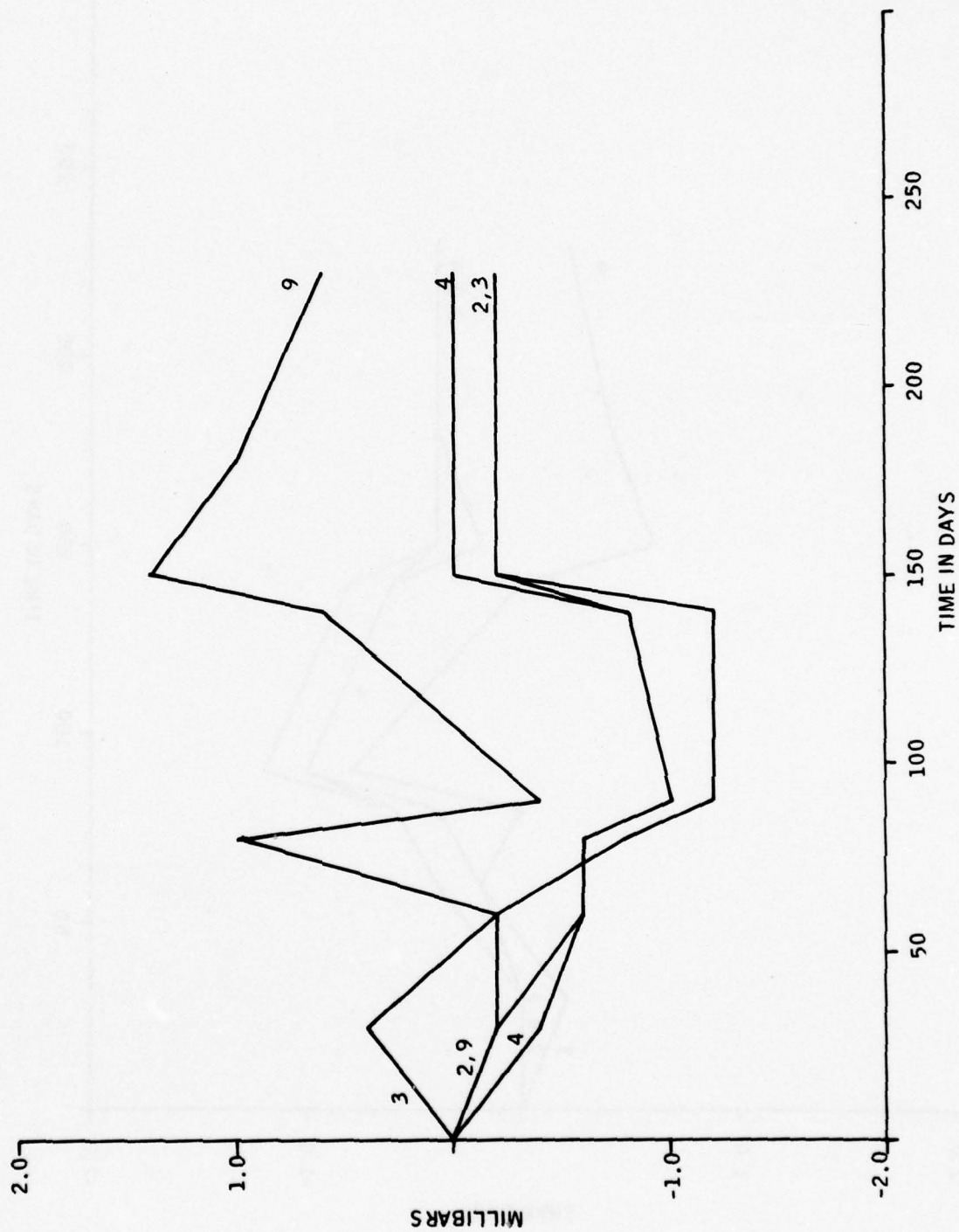


Figure 34. Barometer Drift Data (200 mB, 0°C, S/N's 2,3,4,9)

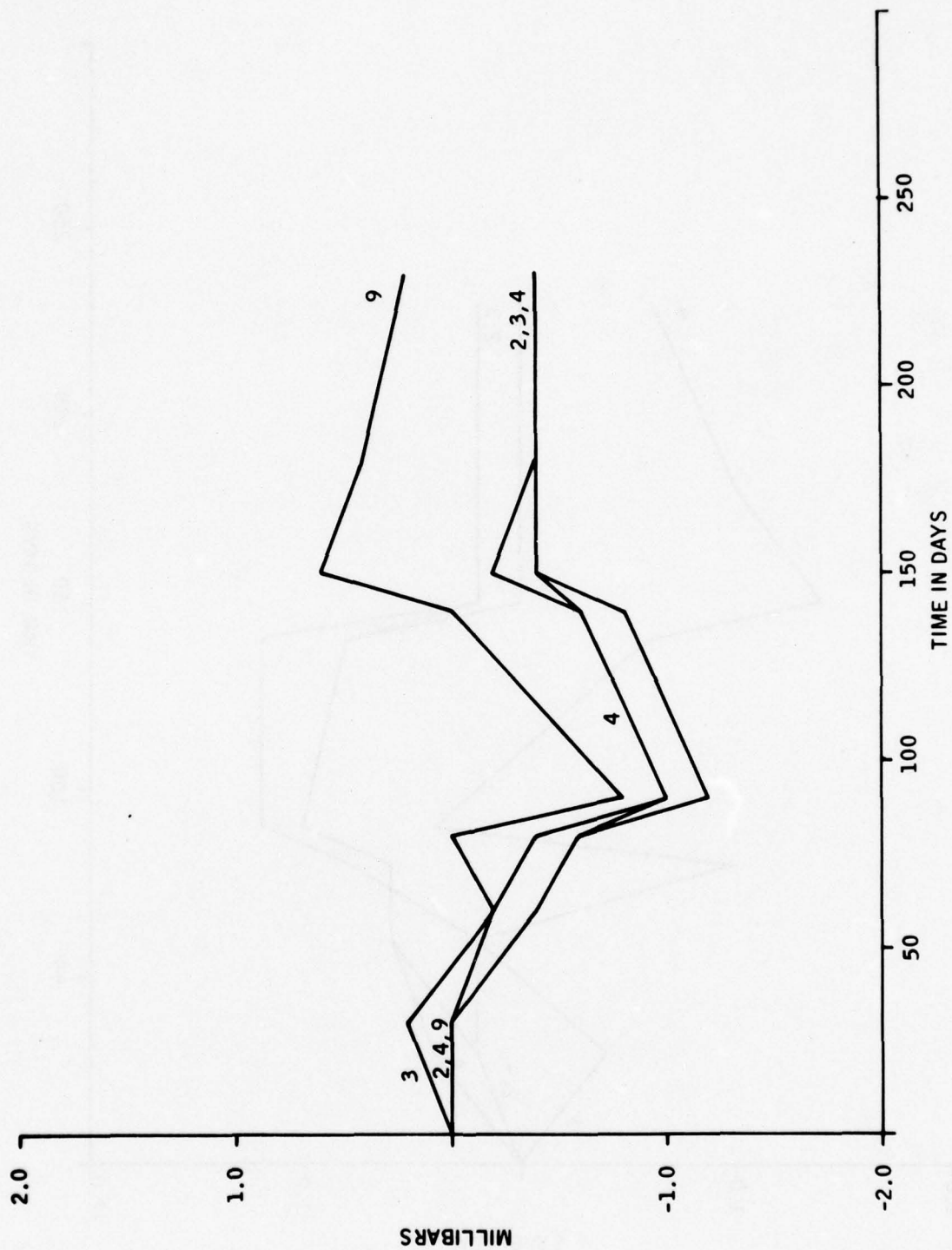


Figure 35. Barometer Drift Data (100 mB, 0°C, S/N's 2,3,4,9)

The minisonde requires a current of approximately 120 milliamperes when operated from a 12-volt supply. The transmitter appears as a resistive load of approximately 110 ohms. The transmitter draws about 100 milliamps and the meteorological electronics draws a constant current of about 15 millamperes.

There tends to be a conflict in the battery requirements because of the two characteristics of light weight and high current drain. In general, a physically small battery is designed to provide a low current drain. For typical applications when a high current drain is required a large battery is used. In our case, we have the advantage that a short operating lifetime is required. Based on a balloon ascent rate of 800 feet per minute and a maximum of about 20,000 feet, a 30-minute lifetime for the sonde is sufficient.

The meteorological electronics require a voltage of 8.5 volts at the battery end-of-life. This establishes the basic battery requirement as a voltage of 8.5 volts at the end-of-life and an initial current capability of 120 milliamperes.

The requirements for a lightweight battery and long operating lifetime are somewhat interrelated. To enable the minisonde to operate longer, a larger and heavier battery with greater capacity could be used. But that would mean that the balloon would rise more slowly and would require a longer period of time to reach the desired 20,000-foot altitude. This would require, therefore a longer battery lifetime. The only real improvement is to have a battery with a greater energy-to-weight ratio. Several types of batteries have been considered for the minisonde application. Many of the more common types, such as the water-activated batteries, zinc-carbon batteries, alkaline and nickel-cadmium cells, are too heavy for the energy required. Only the lithium chemistry type of cell appears to provide the required combination of power density, long storage life, low-temperature operation and light weight.

The sonde must be capable of operating over a temperature range of +50 to -50°C. The energy output, and thus lifetime, of the lithium cells degrades considerably below 0°C. A solution to this life problem at low temperatures is to make the sonde case of an insulating material such as foamed plastic, which will insulate the electronics from the outside air temperature. The heat of the telemetry transmitter is sufficient to keep the internal temperature about 0°C.

The most common form of the lithium family of batteries is the lithium sulfur dioxide cell. These cells are characterized by a high energy-to-weight ratio, good storage life and high output voltage. One problem with the early forms of lithium sulfur dioxide cells was that they could explode when shorted, particularly if they were operating at high temperature. This problem has been overcome by use of different case designs. Another solution was to use a different chemistry, the lithium organic family of cells. These cells do not show the characteristic of exploding when shorted — some have been tested and certified for shipment through the U.S. mails.

One type of cell considered is the Honeywell G3060 lithium cell, which uses the lithium-vanadium pentoxide chemistry. This cell is a flat disc 0.15-inch thick and 1.0-inch diameter. This cell meets the requirements of small size and weighs only 6 grams, yet has the capability of delivering the required current drain.

2. Battery Life

To determine the life characteristics of the G3060 cell under actual flight conditions, a dynamic test was designed. A single cell was placed in the insulated electronics compartment of the minisonde. The electronics were energized and the cell loaded to 120 milliamps. The sonde was placed in a temperature chamber that could be cooled at a known rate to simulate the decrease in air temperature after sonde launch. A temperature lapse rate of 1.2°C per minute was selected to match the atmospheric lapse rate of approximately 2°C per thousand feet.

The sonde and cell were cooled while operating and the cell voltage and electronics temperatures were measured, as shown in Figures 36 and 37. In Figure 36 the sonde was stabilized at a temperature of 80°F prior to the test. Note that the temperature of the transmitter rose to the highest temperature because it was the primary temperature source. The lower curve of Figures 36 and 37 illustrates the free air temperature around the sonde as a function of time. In the second test, the sonde and cell were soaked to stabilize at a temperature of 0°C or 32°F. After launch, the battery temperature increased above 0°C and did not decrease back to 0 until about 34 minutes after the beginning of the test. This would indicate that the desired cell life is obtained.

Based on an 8.5-volt battery end-of-life and five cells per battery, the cell end-of-life is 1.7 volts. As shown in Figure 37, starting at a 0°C launch temperature, the cell voltage did not fall below 1.7 volts until 40 minutes after activation. This is sufficient for the desired flight time.

The G3060 cell is being developed by the Honeywell Power Sources Center for powering electronic watches. A problem developed in the manufacturing process in producing the desired low series resistance. With the higher internal resistances, the desired flight time was not possible. This forced us to consider an alternate battery.

Another lithium battery, designated LR-1/2A, using an organic type electrolyte has recently become available from the Matsushita Electric Company. This cell is 0.5-inch diameter, 0.7-inch long and weighs 9 grams per cell. The series resistance of the LR-1/2A is greater than the G3060, thus giving a lower operating voltage; however, it is still satisfactory for the sonde requirement. The operating life of the cell was determined at three different temperatures, Figure 38. This chart shows that a five-cell battery would easily provide the desired 40-minute lifetime as long as the cell temperature remains above 0°C, which is the condition that will be encountered in an actual sonde case. A five-cell battery using the national LR-1/2A cell will weigh approximately 45 grams, which is significantly higher than the desired 30 grams — however, still within the lifting capacity of a 30-gram balloon. A battery composed of five national LR-1/2A cells will be used in the five minisondes being constructed for this series of tests.

C. METEOROLOGICAL ELECTRONICS

1. Circuit Description

Figure 39 is the circuit diagram of the meteorological electronics used in this series of tests. The meteorological electronics perform the function of switching or commutating between the three sensors and the function of voltage-to-frequency conversion to encode the data for telemetry to the ground.

The commutation function is provided by the integrated circuit, U1, which is a 20-hertz oscillator providing a frequency for switching the sensors. The divider, U2, is used to provide the binary signal to operate the MOS switch U3. U3 is a linear switch connecting, in sequence, the high reference temperature, pressure and the relative humidity voltages to the voltage-to-frequency converter. The integrated amplifier, A1, buffers the sensors from the voltage-to-frequency converter U4. U4 is an integrated voltage-controlled oscillator that has the characteristic of being linear with voltage. U4 provides an output frequency, which is linearly proportional to input voltage with an accuracy of 0.1 percent. The output of U4 is a pulse in the 400- to 4000-hertz range. This signal is divided by 2 in the decade counter U2 to give an output frequency of 200 to 2000 hertz. This frequency is used to frequency-modulate the 400 to 406 megahertz telemetry transmitter. Transistor Q1 and Zener diode D1 regulate the supply voltage at 8 volts.

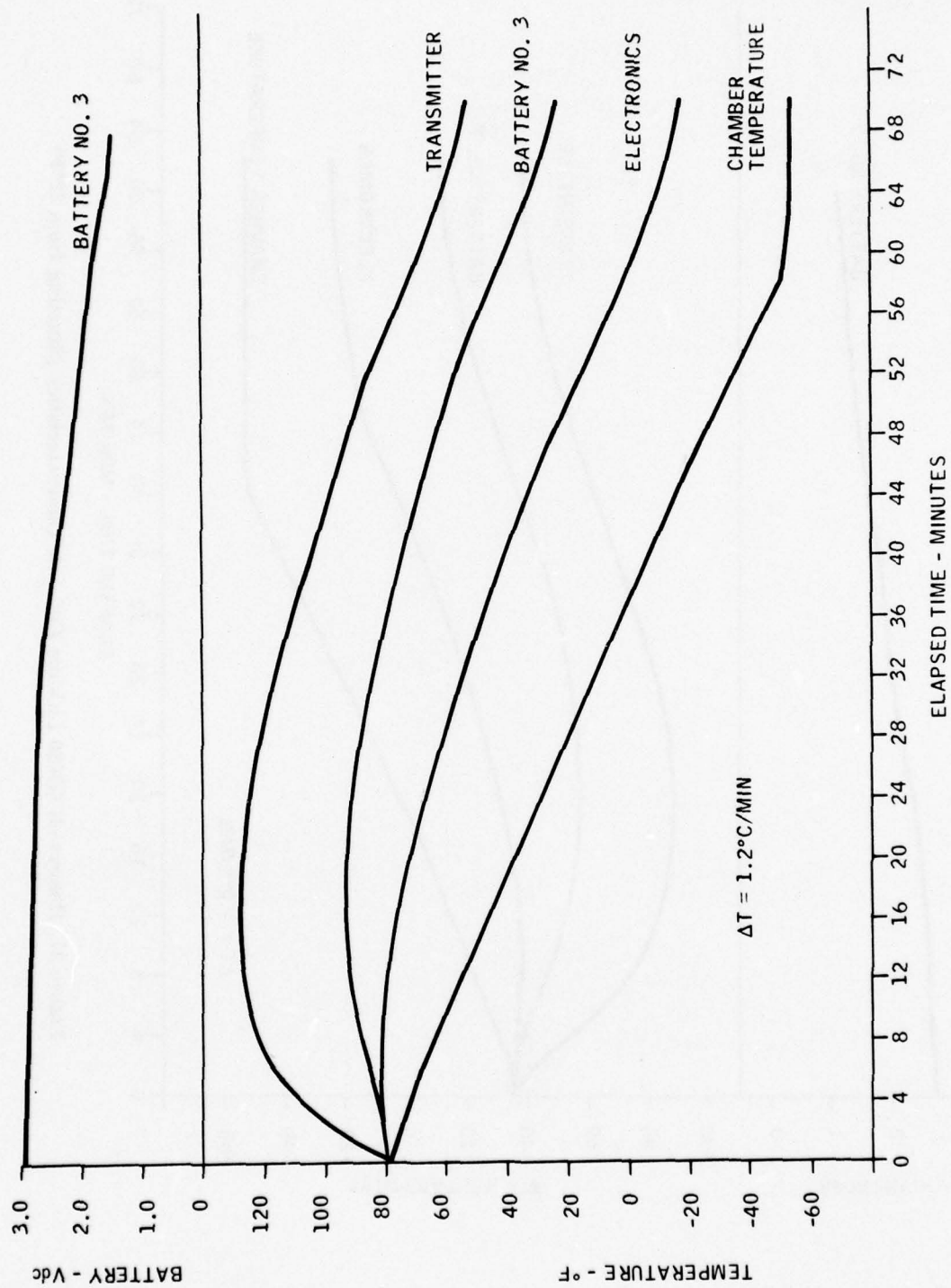


Figure 36. Honeywell G3060 Lithium Cell Life Characteristics (Starting from 80°F)

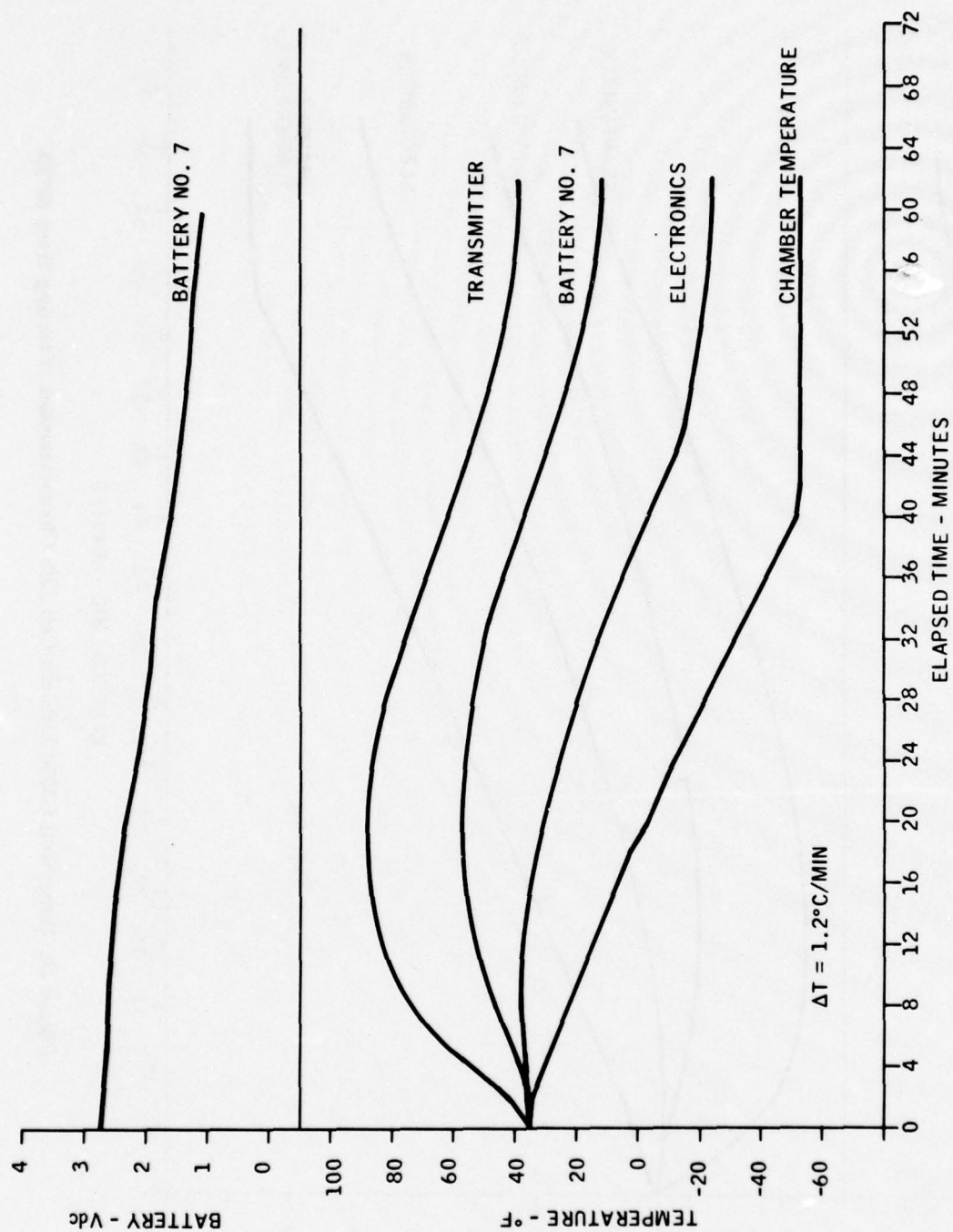


Figure 37. Honeywell G3060 Lithium Cell Life Characteristics (Starting from 32°F)

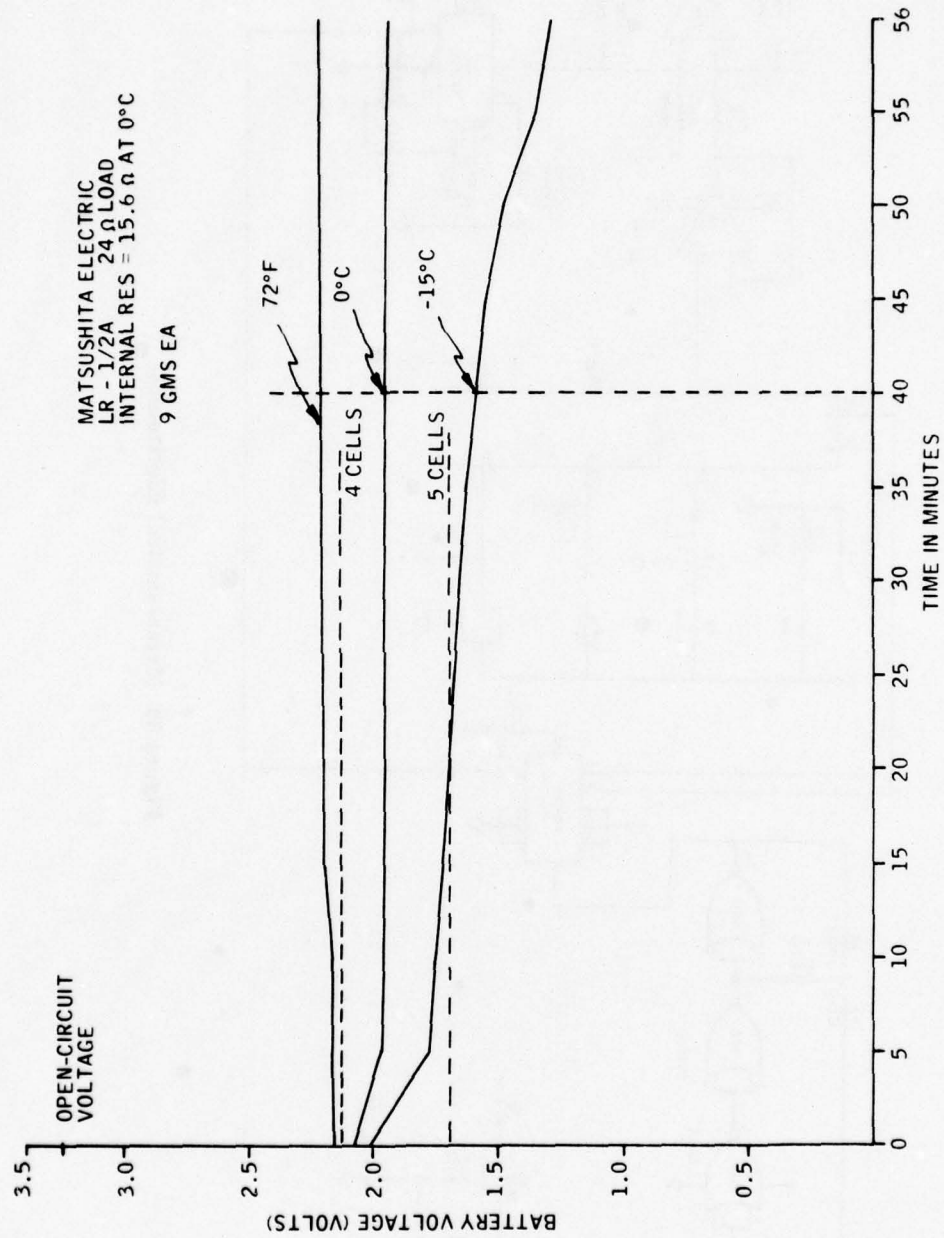


Figure 38. Battery Characteristics

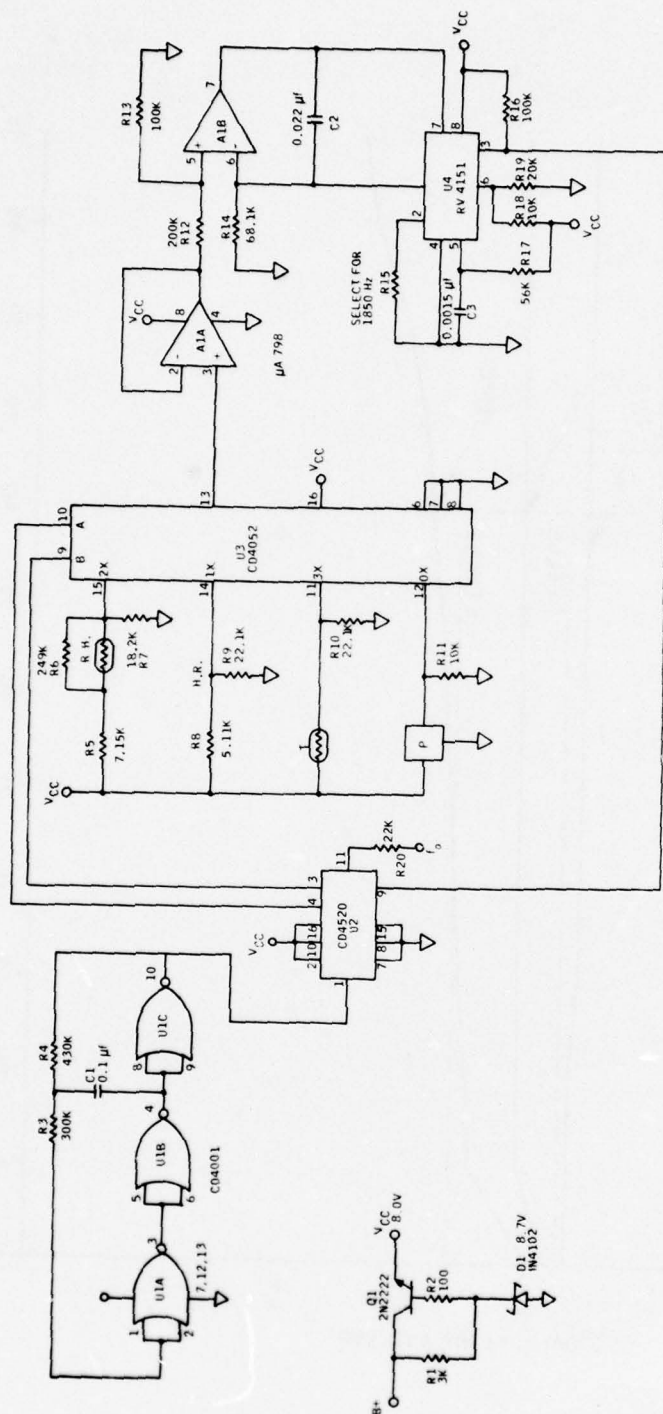


Figure 39. Meteorological Electronics

2. Linearity

To accurately telemeter the meteorological sensor signals to the ground processor it is necessary to accurately encode the sensor signals. The voltage-to-frequency encoder must be accurate to 0.1 percent. The voltage-to-frequency converter must have either an exact relationship between voltage and frequency or the transfer function must be calibrated so that it can be calculated. The 4151 circuit used in the mini-sonde has a linear transfer function providing an output frequency that is linearly related to the input voltage with a curve that passes through zero frequency at zero voltage. The absolute value of frequency at any voltage may change with temperature and supply voltage, but the voltage-to-frequency relationship is linear. To calibrate the telemetry signal a known high reference voltage is encoded periodically.

The deviation from linearity on five voltage-to-frequency converters on five sets of meteorological electronics was measured. The plots are shown in Figures 40 to 44. These curves show the deviation from a straight line curve fit. In each case the high reference frequency was 6.5 volts and the curve was constrained to pass through that point. The linearity was measured over the temperature range from -20° to $+50^{\circ}\text{C}$. Over the voltage range of 1 volt to 6.5 volts the curves are linear within 0.1 percent, which is the desired goal.

To calibrate the voltage-to-frequency converter signal a known high reference voltage is established. This voltage is determined by a precision resistor divider, determined by resistors R8 and R9 in Figure 39. The high reference voltage is the largest signal fed to the oscillator. When the signal is decoded the high reference frequency establishes the voltage-to-frequency conversion line and all the other signals can be proportionately decoded. It is important that the high reference divider ratio remain accurate over temperature. The variation and high reference ratio with temperature is shown in Figure 45. Over the range from 0 to 50°C the temperature-induced ratio variation was 0.06 percent or approximately 3 millivolts. This is within the desired accuracy of 0.1 percent.

The variation in supply voltage with temperature is shown in Figure 46. Since supply voltage variations are corrected by the high reference frequency it is not necessary that the supply voltage be closely regulated.

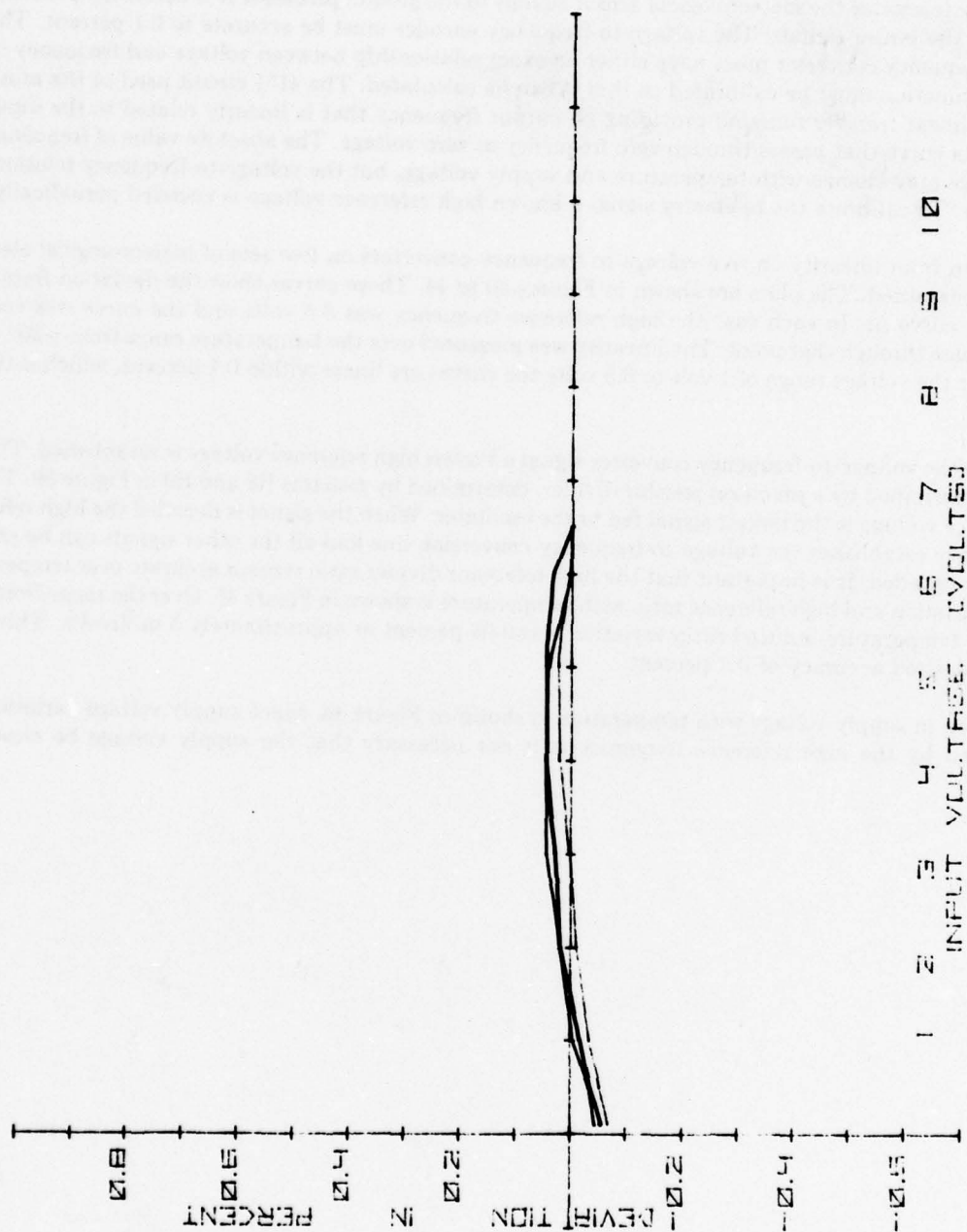


Figure 40. Shows Linearity of the Minisonde Voltage to Frequency Conversion for Five Final Models (Unit No. 7)

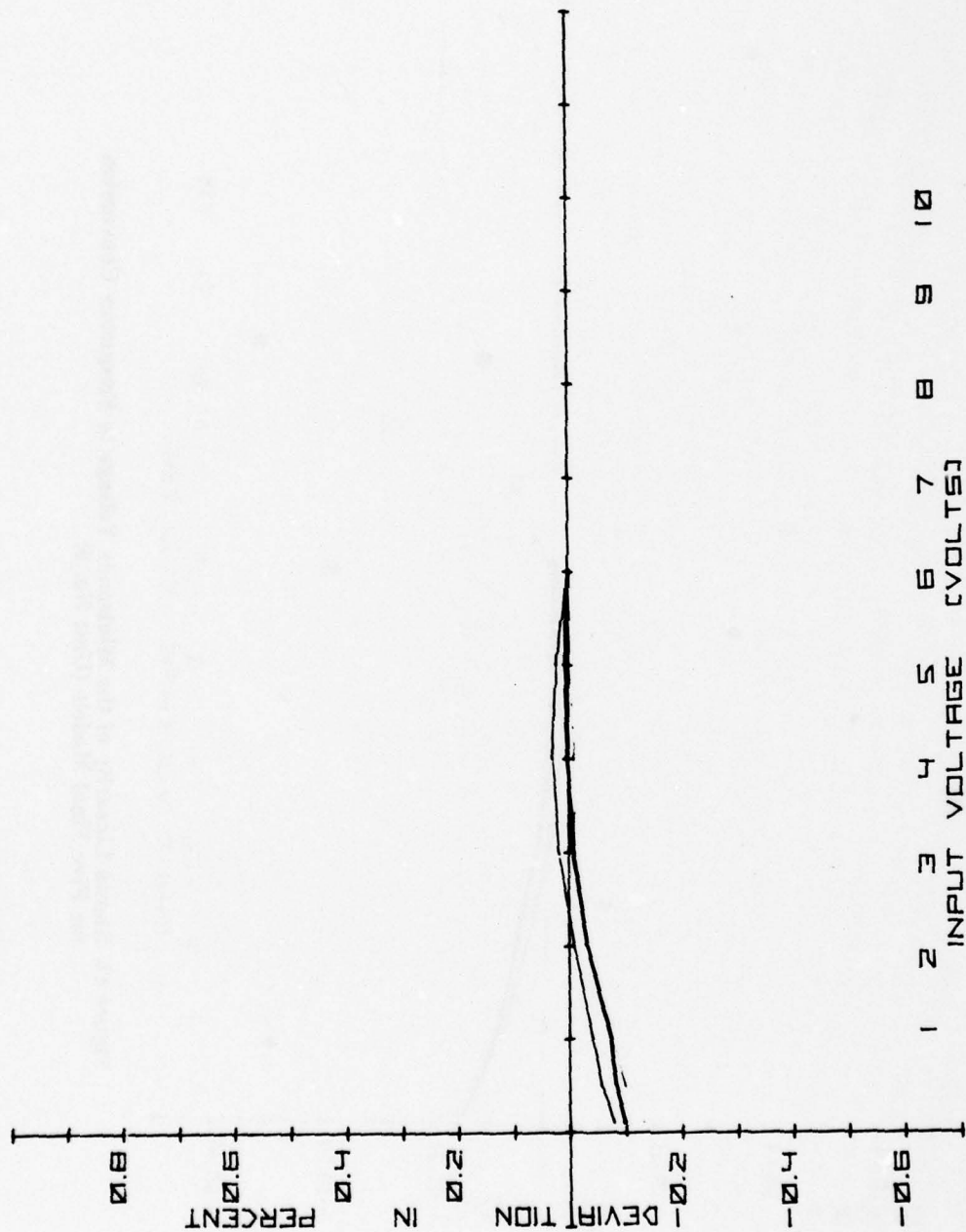


Figure 41. Shows Linearity of the Minisonde Voltage to Frequency Conversion for Five Final Models (Unit No. 8)

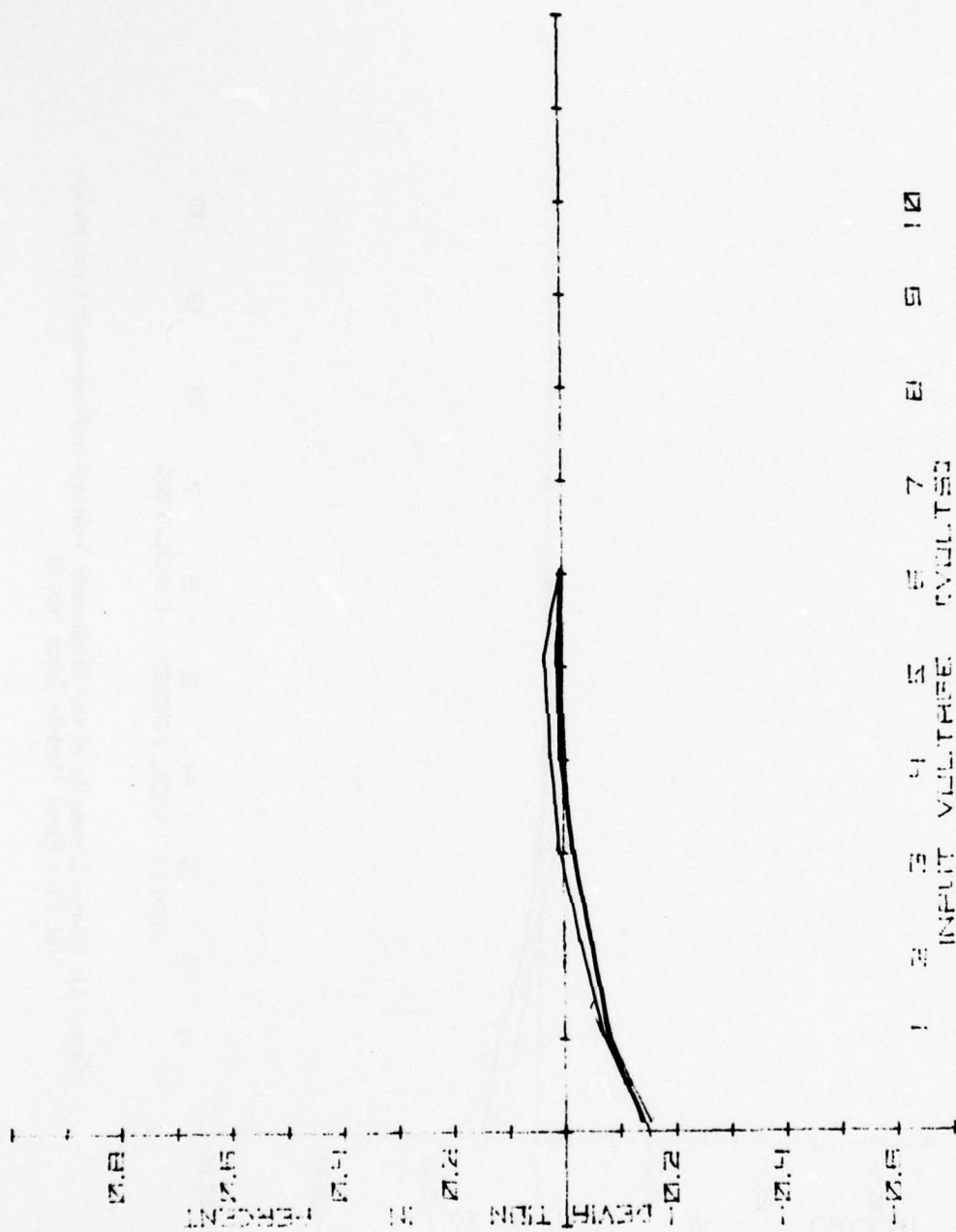


Figure 42. Shows Linearity of the Minisonde Voltage to Frequency Conversion for Five Final Models (Unit No. 9)

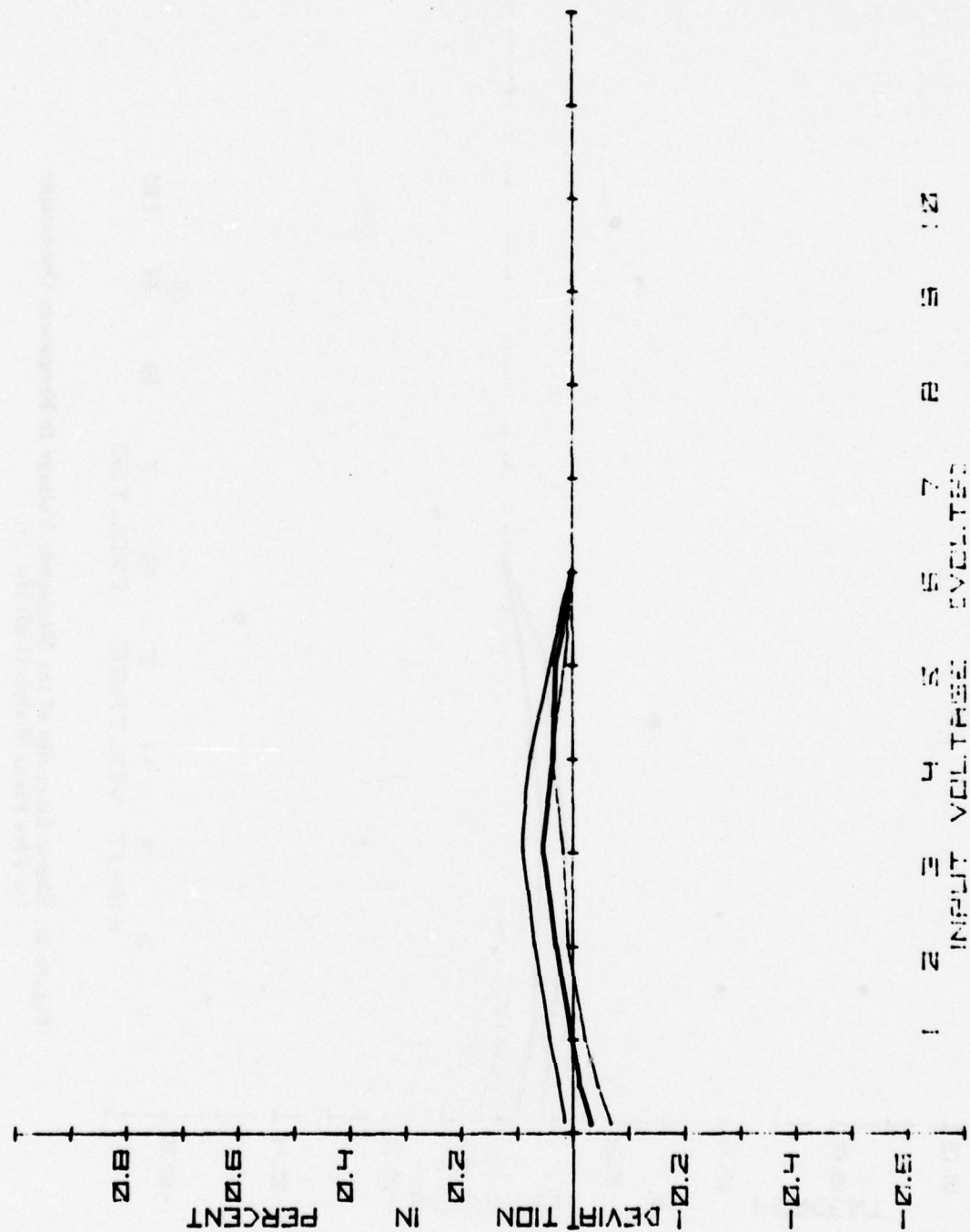


Figure 43. Shows Linearity of the Minisonde Voltage to Frequency Conversion for Five Final Models (Unit No. 10)

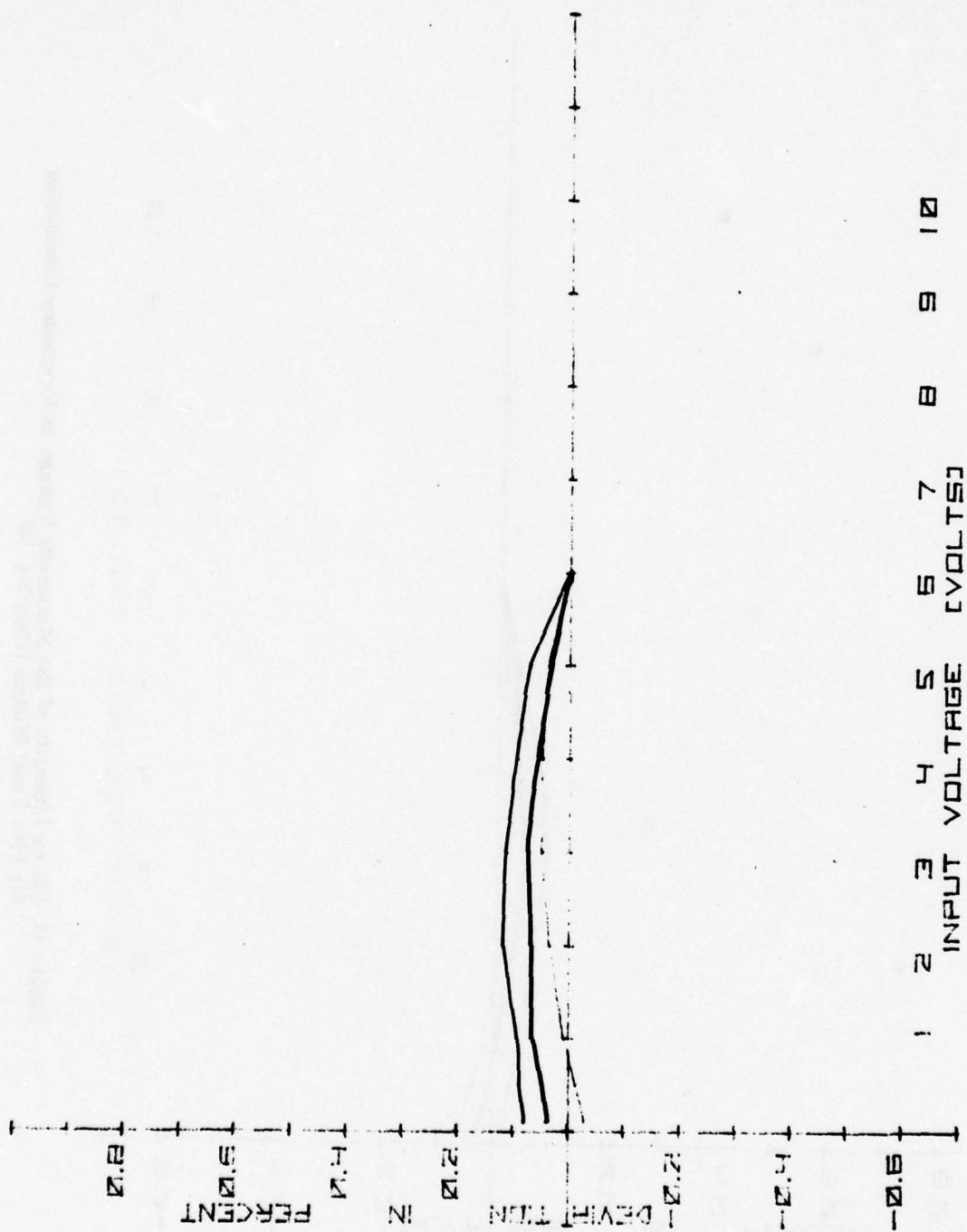


Figure 44. Shows Linearity of the Minisonde Voltage to Frequency Conversion for Five Final Models (Unit No. 11)

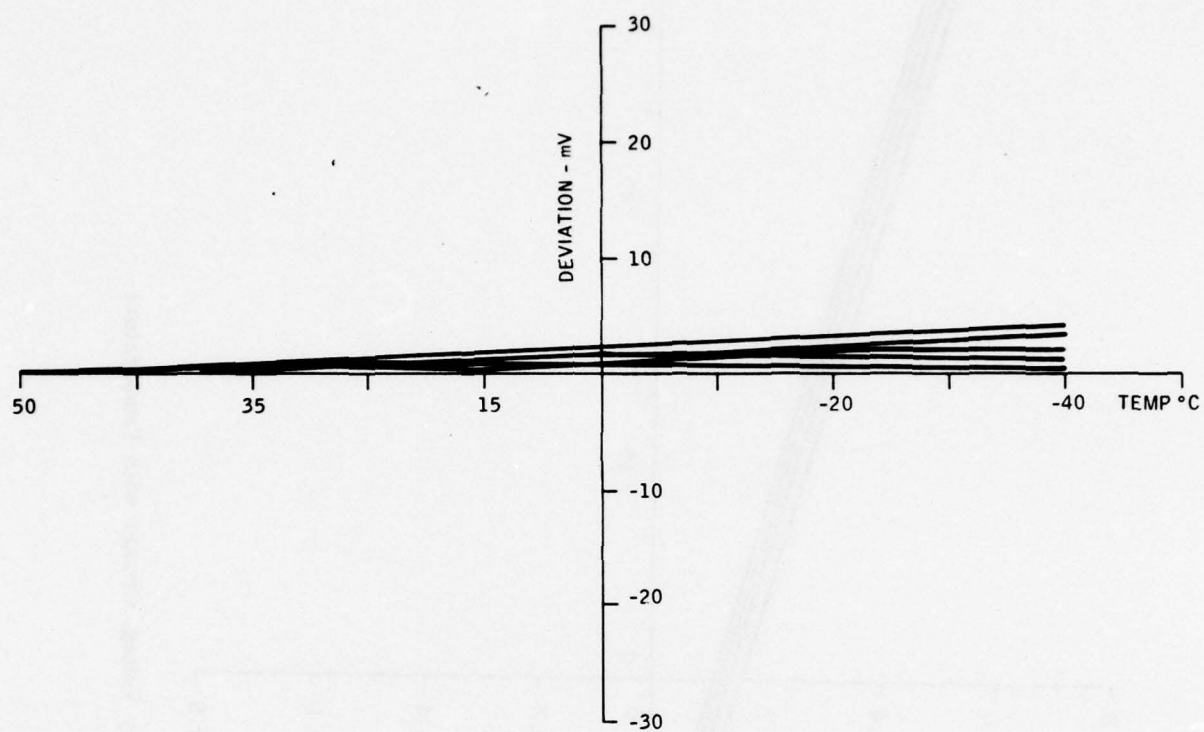


Figure 45. High Reference Stability versus Temperature

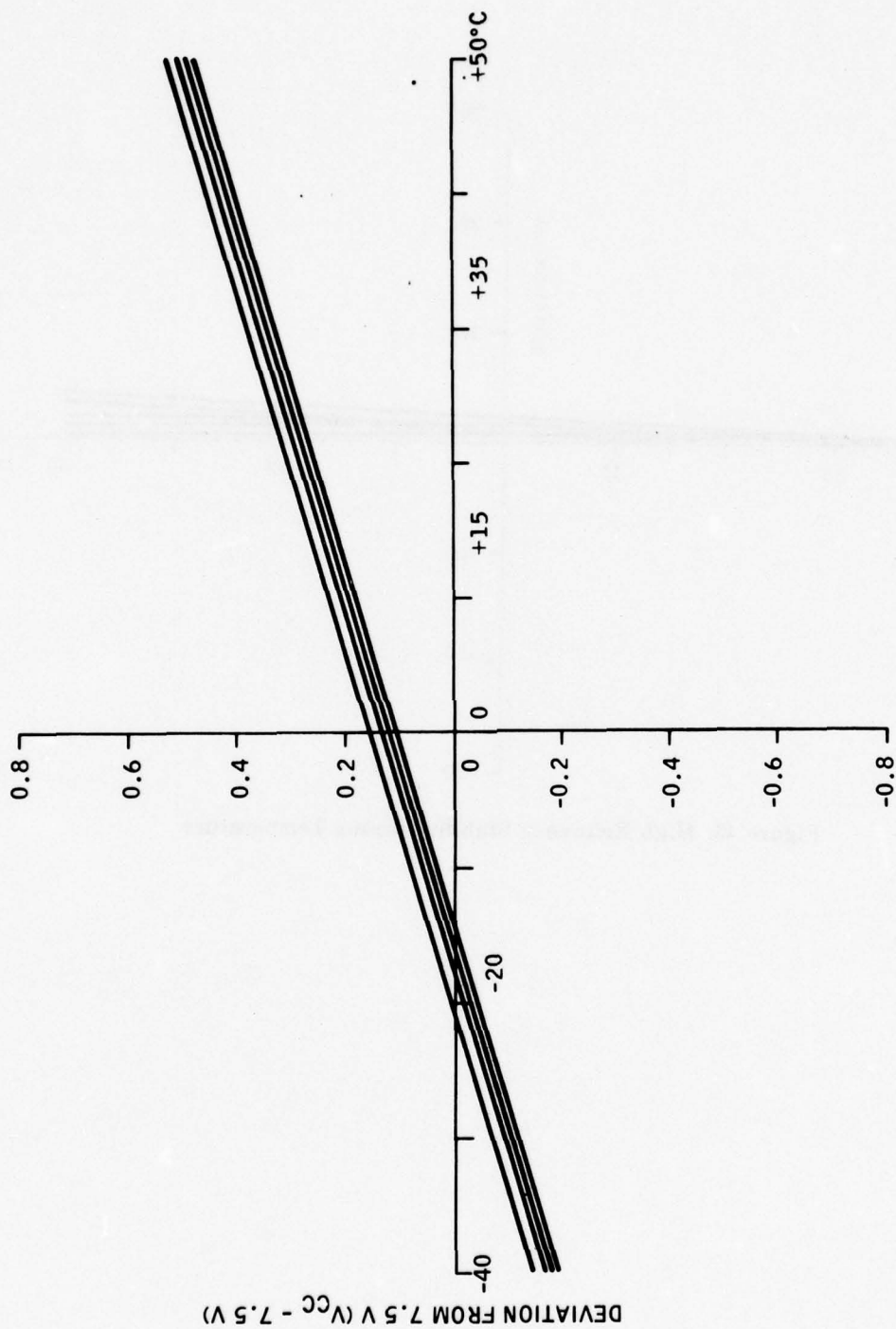


Figure 46. Supply Voltage Change with Temperature

III. Laboratory Tests on the Mini-Refractiionsondes

A. DATA REDUCTION

The minisonde sensors provide a voltage signal that is converted to frequency by the Voltage-Controlled Oscillator (VCO). This frequency is telemetered to the ground processor where it is decoded to obtain temperature and humidity versus altitude readings. The data reduction procedure is as follows:

- Convert from frequency (200-2,000 hertz) to voltage (0.6-6 volts) using the voltage-to-frequency transfer function of the minisonde VCO.
- For temperature and humidity, convert from voltage to resistance using the sensor resistance network transfer function.
- Convert from resistance to temperature or humidity using the sensor conversion equations.
- For pressure, convert from voltage to pressure using the solid-state barometer transfer function.
- Convert from pressure to altitude using the barometric equation.

1. Frequency-to-Voltage Conversion

The voltage-to-frequency conversion is accomplished in the minisonde by a Voltage-Controlled Oscillator (VCO). The VCO has a linear transfer function that passes through the origin. Thus, VCO output can be described by the equation $y = mx$.

Since the offset from the origin is essentially zero over temperature and supply voltage, only one point on the curve is required to define the value of m . The high reference frequency (see high reference below) fixes this point and calibrates any variations due to temperature and supply voltage. The conversion equation is:

$$f = mV$$

$$m = \frac{f_{HR}}{V_{HR}} \quad (2)$$

where:

V_{HR} = High reference voltage
 f_{HR} = High reference frequency
 f = Output frequency
 V = VCO voltage

Figures 40 through 44 show percent of deviation from the straight line $f = mV$ where the deviation is less than 0.1 percent.

2. Supply Voltage and High Reference

Supply voltage (V_{CC}) is held constant by the regulator circuit of Q1 (Figure 39). The high reference (HR) voltage is obtained from the resistor divider network R8 and R9 as shown in Figure 39. The ratio is chosen so that the HR voltage will be higher than the voltage from any of the sensors.

The high reference ratio is:

$$V_{HR} = \frac{R_9 V_{CC}}{R_8 + R_9} = 0.8122 V_{CC} \quad (3)$$

Therefore:

$$m = \frac{f_{HR}}{V_{HR}} = \frac{f_{HR}}{0.8122 V_{CC}} \quad (4)$$

3. Temperature

There are three steps in the calculation of free air temperature from the telemetered frequency: conversion from frequency to voltage, conversion from voltage to resistance and conversion from thermistor resistance to temperature. The thermistor voltage (V_T) is determined by R10 and the thermistor resistance (R_T), as shown in Figure 39.

$$V_T = \frac{R_{10} \times V_{CC}}{R_{10} + R_T} = \frac{22100 V_{CC}}{R_T + 22100} \quad (5)$$

From Equation (2):

$$V_T = f_T/m \quad (6)$$

where:

V_T = Voltage from thermistor divider

f_T = Frequency output from thermistor voltage

And from the high reference Equation (4)

$$V_{CC} = \frac{f_{HR}}{0.8122 m} \quad (7)$$

Substituting Equation (6) and (7) in (5) and solving for thermistor resistance R_T gives:

$$R_T = \frac{27210 f_{HR}}{f_T} - 22100 \quad (8)$$

where:

f_{HR} = High reference frequency

f_T = Thermistor frequency

The equation for the calculation of temperature requires the ratio of the thermistor resistance to that of the thermistor resistance at +30°C, therefore:

$$r = \frac{R_T}{R_{T0}} \quad (9)$$

where:

r = Resistance ratio

R_T = Resistance of thermistor in ohms

$R_{T0} \approx 14,000$ = thermistor lock-in resistance

An equation for calculating temperature from resistance ratio as shown in Equation (10) was provided by Mr. S. Grillo of the Naval Air Development Center.

$$T = \sqrt{\left[\frac{240.5}{A} - (273.15)^2 + B^2 \right]} - B \quad (10)$$

where:

$$A = \ln \left[\frac{r}{3.379 (10)^{-4}} \right]^{1/2715.6}$$

$$B = \frac{546.32 A - 1}{2A}$$

Another equation for conversion from resistance ratio to temperature is given by Technical Publication 761101B from the VIZ Manufacturing Company.

The following third order polynomial equation converts sensor resistance to temperature (degrees celsius). The equation and constants, developed for use with VIZ premium temperature sensors (used in projects such as IFYGL and GATE), provide an almost perfect match ($\pm 0.01^\circ\text{C}$) to the nominal sensor test data.

$$t = \frac{1}{\sum_{k=0}^3 A_k [\ln(R_t/R_{30})]^k} - 273.15 \quad (11)$$

$$A_0 = 3.2987 \text{ E-03}$$

$$A_1 = 4.7764 \text{ E-04}$$

$$A_2 = 3.0029 \text{ E-06}$$

$$A_3 = 1.5108 \text{ E-06}$$

R_t = Temperature sensor resistance

R_{30} = Temperature sensor lock-in resistance at +30°C. (See Note 1).

Ratio = R_t/R_{30}

Temp. °C	Ratio	Temp °C	Ratio	Temp. °C	Ratio
50*	0.652	0	2.124	-50	10.98
40	0.802	-10	2.827	-60	16.40
30	1.000	-20	3.838	-70	25.22
20	1.265	-30	5.322	-80*	40.00
10	1.626	-40	7.551	-90*	65.59

Note 1. The nominal value is 14,000 ohms. R₃₀ is provided with the VIZ ACCU-LOK sensors (1266-211) and the VIZ ACCU-LOK premium sensors (1366-211).

*Extrapolated values.

4. Humidity

Humidity is sensed with a variable resistance carbon hygistor. Because of the wide range of resistance change of the carbon hygistor a series resistance of 7.15K (R₅) and a shunt resistance of 249K (R₆) are used to limit the minimum values (Figure 39). An equivalent resistance R_X can be defined equal to the network of R₅, R₆, and R_H.

$$R_X = R_5 + \left[\frac{R_6 \times R_H}{R_6 + R_H} \right] \quad (12)$$

Following the data reduction procedure developed for the temperature measurement, the humidity voltage V_H is:

$$V_H = \frac{R_7 \times V_{CC}}{R_7 + R_X} = \frac{18200 V_{CC}}{18200 + R_X} \quad (13)$$

From Equation (2):

$$V_H = f_{RH}/m \quad (14)$$

where f_{RH} is the humidity sensor signal frequency.

Substituting Equation (7) for V_{CC} and Equation (14) for V_H in Equation (13) and solving for R_X:

$$R_X = \frac{22408 f_{HR}}{f_{RH}} - 18200 \quad (15)$$

Solving Equation (12) for the resistance (R_H) of the carbon hygistor:

$$R_H = \frac{R_6 (R_X - R_5)}{R_6 + R_5 - R_X} \quad (16)$$

Substituting values for R5 and R6:

$$R_H = \frac{24900 R_X - 1.7704 (10)^9}{256150 - R_X} \quad (17)$$

Substituting the value for R_X gives the hygistor resistance.

The relative humidity (RH) with respect to water can be calculated using the expressions from "Humidity Sensor Transfer Equations," VIZ Manufacturing Co. Technical Publication No. 761102A.

$$RH_W = A - \frac{1}{D_0 + D_1 G + D_2 G^2 + D_3 G^3 + D_4 G^4} \quad (18)$$

and:

$$G = [C_0 + C_1 t + C_2 t^2] \ln (R_H/R_{33}) \quad (19)$$

where:

RH_W = Percent relative humidity with respect to water

R_H = Humidity sensor resistance

R_{33} = Humidity sensor lock-in resistance (33 percent RH_W and $+25^\circ\text{C}$)

t = Temperature in $^\circ\text{C}$

The nominal lock-in value (R_{33}) is 10,000 ohms. R_{33} is provided with the VIZ ACCU-LOK sensors (1286-060) and the VIZ ACCU-LOK premium sensors (1386-060). For baseline procedures, see Technical Publication 761104.

The constants for Equation (19) are:

For $R_H/R_{33} \geq 1.000$

$$C_0 = 8.507 \text{ E-1}$$

$$C_1 = 5.733 \text{ E-3}$$

$$C_2 = 9.587 \text{ E-6}$$

For $R_H/R_{33} < 1.000$

$$C_0 = 9.243 \text{ E-1}$$

$$C_1 = 3.059 \text{ E-3}$$

$$C_2 = -1.188 \text{ E-6}$$

The constants for Equation (18) are:

For $G \geq -0.2$

$$\begin{aligned} D_0 &= 1.3889 \text{ E-2} \\ D_1 &= 9.3991 \text{ E-3} \\ D_2 &= -5.0689 \text{ E-4} \\ D_3 &= 2.0415 \text{ E-5} \\ D_4 &= 2.0811 \text{ E-4} \\ A &= 105 \end{aligned}$$

For $G < -0.2$

$$\begin{aligned} D_0 &= -3.0303 \text{ E-2} \\ D_1 &= 6.4307 \text{ E-2} \\ D_2 &= -8.2662 \text{ E-2} \\ D_3 &= -9.4366 \text{ E-2} \\ D_4 &= -3.7479 \text{ E-1} \\ A &= 0 \end{aligned}$$

Nominal Resistance Ratio —

R_g/R_{33} at the given RH_W and temperature

RH _W	+40°C	+25°C	0°C	-20C	-40°C
10	0.608	0.595	0.570	0.548	0.522
20	0.798	0.790	0.775	0.761	0.745
30	0.945	0.943	0.939	0.934	0.929
33	1.000	1.000	1.000	1.000	1.000
40	1.157	1.174	1.207	1.242	1.286
50	1.531	1.595	1.731	1.879	2.082
60	2.305	2.496	2.930	3.443	4.206
70	4.137	4.735	6.221	8.179	—
80	8.644	10.61	16.06	24.34	—
90	21.31	28.50	51.31	—	—
100	112.0	175.3	—	—	—

Another humidity algorithm has been derived by Merv Werst of Analytics Corp. This provides a simple expression with a 1-2 percent fit to the data table. The expression is:

For $r \geq 1$

$$RH_W = 33 + A [\ln (r^B)]^C \quad (20)$$

where:

$$A = 0.02t + 3.2$$

$$B = 15$$

$$C = 0.9 - [0.001425t + 0.25] \{ \log_{10} (\log_{10} r + 1) \}^{1/3}$$

For $r < 1$

$$RH_W = 33 - A [\ln (r-B)]^C \quad (21)$$

where:

$$A = 0.02t + 3.2$$

$$B = 20$$

$$C = 0.9 - [0.001425t + 0.25] \{ \log_{10} (\log_{10} r^{-1} + 1)^{1/3} \}$$

RH_W = Relative humidity with respect to water

$$r = R_H/R_{33}$$

$$t = \text{Temperature in } ^\circ\text{C}$$

5. Pressure and Altitude

Calculation of altitude requires pressure at the altitude as well as the temperature and humidity profile below the sonde. To calculate pressure, from Equation (2):

$$V_B = \frac{f_B}{m} \quad (22)$$

where:

V_B = Voltage signal from the barometer

f_B = Frequency of barometer signal

Using Equations (3) and (4), and substituting for m in Equation (22) gives:

$$V_B = \frac{0.8122 V_{CC} f_B}{f_{HR}} \quad (23)$$

Barometer pressure can now be calculated from Equation (1) using V_B from Equation (23), free-air temperature and measured V_{CC} . The high reference ratio and V_{CC} were measured for each sonde as shown in Table 1 and Figure 46.

Altitude can now be calculated using the following equations for geopotential height as provided by Mr. Ken Anderson of Naval Ocean System Center.

The objective is to compute the values for HT_i , N_i and M_i where:

HT_i = Height in geopotential meters at level i

N_i = Modified refractive index at level i

M_i = M-unit value at level i

P_i = Pressure in millibars at level i

T_i = Temperature in degrees celsius at level i

T^* = Virtual temperature in $^\circ\text{C}$

RH_i = Relative humidity in percent at level i

TABLE 1. SONDE CALIBRATION DATA

Sonde Number	Thermistor Lock-In	Barometer Number	High Reference Ratio to 0°C
7	14,101	380005 (BN10)	0.8119
8	14,237	380009 (BN8)	0.8131
9	13,561	380010 (BN7)	0.8123
10	13,704	380043 (BN1)	0.8127
11	13,955	380026 (BN5)	0.8137

VCC = 7.7 V at 0°C
 Calculated High
 Reference Ratio = 0.8122

W = Mixing ratio in gm/gm
 E = Vapor pressure in mB
 ES = Saturation vapor pressure in mB
 Level 1 (i=1) = Launch level
 Level 2 (i=2) = Level immediately above launch level
 Level n (i=n) = Maximum (last) level of observation

Starting with i=1, set HT_i equal to the height of the station in meters above mean sea level. Calculate saturation vapor pressure (ES) in mB.

$$ES = 6.105 \text{ EXP } [25.22 \{T_i/(T_i + 273.2)\} - 5.31 \ln (1 + T_i/273.2)] \quad (24)$$

Vapor pressure in mB:

$$E = (RH_i/100) ES \quad (25)$$

Mixing ratio in gm/gm

$$W = 0.62197 \times E/(P_i - E) \quad (26)$$

Virtual temperature in degrees Kelvin:

$$T^* = (1 + 0.61W) (T_i + 273.2) \quad (27)$$

Now compute the height (HT_i) in geopotential meters. On the first step when i = 1 use launch altitude.

$$HT_i = HT_{i-1} + 29.286 \left(\frac{T^* + TMP^*}{2} \right) \ln (P_{i-1}/P_i) \quad (28)$$

The new value of TMP* is:

$$\text{TMP}_i^* = T_{i-1}^* \quad (29)$$

The modified refractive index (N_i) is:

$$N_i = \frac{77.6}{T_i + 273.2} \left[P_i + \frac{4810 E}{T_i + 273.2} \right] \quad (30)$$

and M-units are:

$$M_i = N_i + 0.157 \text{ HT}_i \quad (31)$$

6. Reduction Procedure

The RF signal from the sonde is demodulated to detect the VCO frequency for processing. The demodulated signal is interfaced into a minicomputer where the computer separates the four different commutations:

1. HR
2. Relative humidity
3. Temperature
4. Pressure

If two adjacent data frequencies are the same, a 100-millisecond timing clock will cause the shift to the next commutation instead of the normal change in frequency shift; an asterisk will be generated at that point in the data if this happens. It then counts the number of microseconds required for 10 positive going zero crossings of the signal. This data is transferred to computer data tapes for further processing. A functional flow chart of this procedure is given in Figure 47.

From the data tape, the data is transferred to a data file for processing in a Fortran program MEDARE (MEteorological DAta REDuction), Figure 48. This program incorporates the equations discussed in characteristic equations above.

The program calls for the calibration constants for the sonde whose data is to be processed. It then reads the first frame of data, i.e., the first four commutations HR, RH, T, and P — and converts the 10-cycle time to frequency which is used to calculate temperature, pressure, altitude, and relative humidity. From this information, a tabular output of Altitude, Temperature, Humidity, Pressure, and HR Frequency is printed. The process is repeated for each additional frame of data until the file is exhausted.

B. SONDE MEASUREMENT ACCURACY

To determine the overall sonde system accuracy, a simulated flight test was performed. Sonde number 7 was placed in a temperature- and pressure-controlled chamber and energized with a 12-volt power supply. As the temperature and pressure of the chambers were varied, the met signal was telemetered to a Nems-Clarke 400-406 MHz FM receiver. The demodulated signal was recorded and an analog tape recorded. This signal was then played back through a digitizer into a computer that decoded the signal and calculated temperature, pressure and humidity.

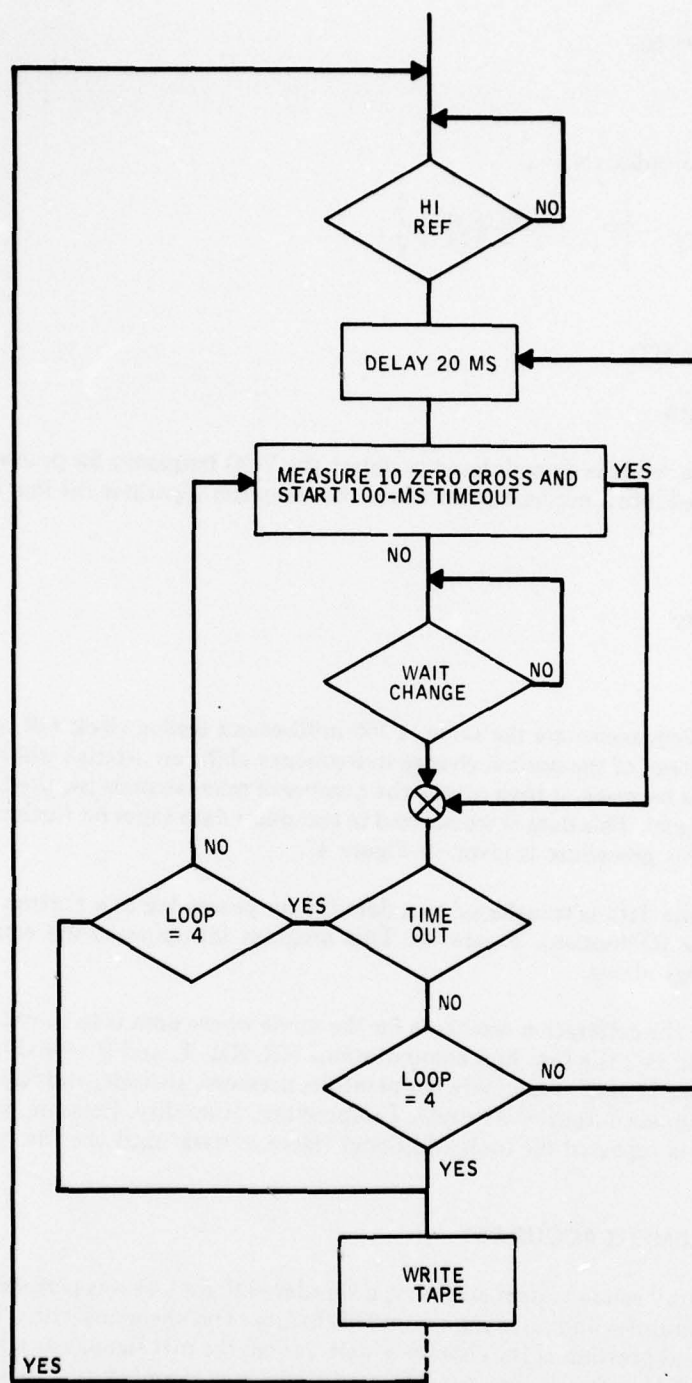


Figure 47. Digitizer Flow Diagram

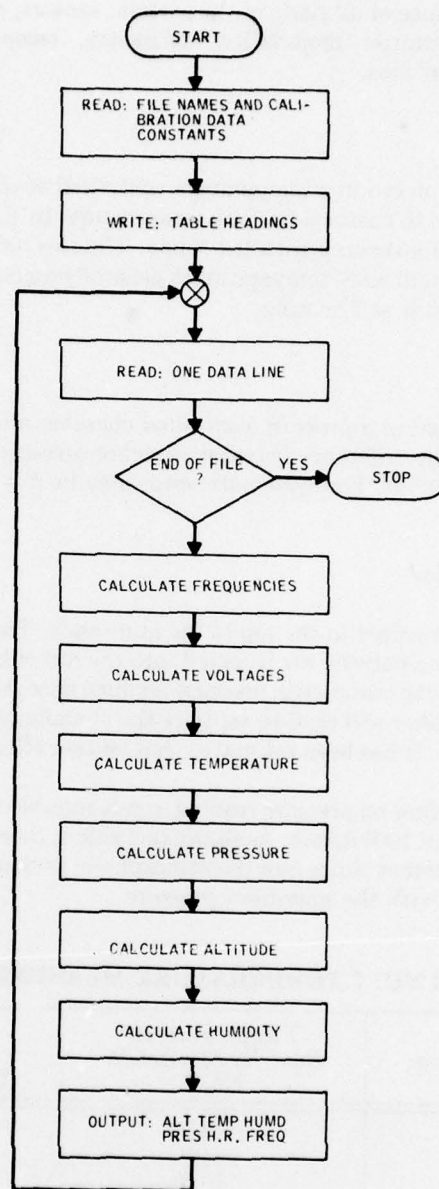


Figure 48. Data Reduction Sequence

This test measures the performance of all parts of the system: sensors, commutation, encoding (voltage-to-frequency conversion), transmitter modulation, telemetry, reception, demodulation, digitizing, decoding and computation algorithms.

1. Temperature

The sonde (number 7) was first placed in a temperature-controlled environmental chamber. A fan in the chamber provided air circulation to ensure a uniform temperature. In Table 2 is shown the chamber temperature versus the temperature measured with the sonde. The rms difference in temperature measurement was 0.45°C. Note that the indicated temperature is generally higher than the chamber temperature. This may be caused by thermistor self heating.

2. Pressure

Next, sonde number 7 was placed in a pressure-controlled chamber and the pressure varied from 300 to 1050 millibars. Table 3 shows the difference between chamber pressure and the sonde reading. The rms pressure difference was 0.59 millibar. The systematic error may be due to the accuracy of the barometer curve fit.

3. Effect of Airflow on Barometer

The barometer is located in a chamber in the top of the minisonde. This chamber is open at the top and sides. As the sonde rises with the balloon, air is forced into the top of the chamber tending to produce a "ram-air" effect and increasing the barometric pressure reading. Also, the air flowing past the openings in the sides of the barometer chamber will tend to aspirate the chamber and reduce the chamber pressure. These effects will tend to cancel. It has been estimated that neither effect will exceed 0.1 millibar change.

To demonstrate the effect of airflow on pressure reading, sonde number 8 was operated with and without a fan, providing an airflow of about 1000 ft/min. As shown in Table 4, there is essentially no effect of airflow. The readings were made at different times and the atmospheric pressure had changed. The telemetered and decoded data agreed well with the measured pressure.

TABLE 2. SONDE NO. 7 TEMPERATURE MEASUREMENT ACCURACY

Chamber Temperature °C	Temperature as Read By Minisonde No. 7	Difference Temperature
50	49.9	-0.1
35	35.0	0.0
15	15.3	0.3
0	0.7	0.7
-20	-19.5	0.5
-40	-39.4	0.6

rms = 0.45°C

TABLE 3. SONDE NO. 7 PRESSURE MEASUREMENT ACCURACY

Chamber Pressure (mB)	Pressure as Read by Sonde (mB)	Difference Pressure (mB)
1050	1050.1	0.1
1000	1000.8	0.8
950	950.4	0.4
900	901.1	1.1
850	850.5	0.5
800	800.3	0.3
750	750.7	0.7
700	700.3	0.3
650	649.9	-0.1
600	600.0	0
550	549.9	-0.1
500	499.5	-0.5
450	449.2	-0.8
400	399.2	-0.8
350	349.3	-0.7
300	299.2	-0.8

rms = 0.59 mB

**TABLE 4. BAROMETRIC PRESSURE MEASURED WITH SONDE NO. 8
WITH AND WITHOUT AIRFLOW**

	With Fan	Without Fan
Atmospheric Pressure (mB)	989.0	990.5
Sonde Measured Pressure (mB)	989.1	990.5
Difference (mB)	0.1	0

4. Telemetry Transmitter

The power output and frequency were measured on all five VHF telemetry transmitters, as shown in Table 5. The power output was about 0.5 watt at full supply voltage and dropped to 0.25 watt at 10 volts supply. Frequency only changed 0.3 MHz on the average.

5. Sonde Calibration Data

For reduction of the sonde telemetry data, the lock-in values are provided in Table 1 on page 60.

6. Balloon Characteristics

To determine the rise rate and maximum altitude that will be achieved with the minisonde launched by a 30-gram pibal balloon, a series of tests were performed by Ralph Sellitsch and Ed Schmidt of NADC. For these tests, groups of balloons were inflated to provide a free lift of 185 to 215 grams. A 90-gram radar reflector was attached to simulate the sonde while the balloon and reflector was launched and tracked with radar. A summary of the 15 launches is tabulated in Table 6. This shows that ascent rates of 600 to 1000 feet per minute can be achieved with burst altitudes of 25,000 to 20,000 feet. Since most of the refractivity data is below 10,000 feet, this performance is satisfactory. These flight results represent a warm, sunny day in November. Results can change ± 20 percent with warmer or cooler weather conditions.

TABLE 5. MINISONDE TELEMETRY TRANSMITTER DATA

	Supply Voltage	Supply Current	Power Output	Frequency
S/N 10	Weight: 13.6 gms			
	At 25°C			
at 13.5 Vdc:	103.7 ma,	26.76 dBm,	404.16 MHz	
at 10.0 Vdc:	72.8 ma,	23.72 dBm,	403.99 MHz	
S/N 11	Weight: 13.2 gms			
	At 25°C			
at 13.5 Vdc:	99.1 ma,	26.56 dBm,	404.10 MHz	
at 10.0 Vdc:	71.0 ma,	23.84 dBm,	403.77 MHz	
S/N 12	Weight: 13.3 gms			
	At 25°C			
at 13.5 Vdc:	107.7 ma,	26.94 dBm,	404.06 MHz	
at 10.0 Vdc:	77.9 ma,	24.16 dBm,	403.79 MHz	
S/N 13	Weight: 13.6 gms			
	At 25°C			
at 13.5 Vdc:	105.6 ma,	26.96 dBm,	404.03 MHz	
at 10.0 Vdc:	77.6 ma,	24.40 dBm,	403.73 MHz	
S/N 14	Weight: 13.3 gms			
	At 25°C			
at 13.5 Vdc:	105.7 ma,	27.13 dBm,	404.08 MHz	
at 10.0 Vdc:	75.2 ma,	24.38 dBm,	403.83 MHz	

**TABLE 6. MEASURED CHARACTERISTICS OF A 30-GRAM
PIBAL BALLOON**

Free Lift	Sonde Weight	Rise Time	Max Alt
185 gms	90	600 ft/min	25K
230 gms	90	800 ft/min	22K
275 gms	90	1000 ft/min	20K

IV. Conclusions

The first phase of the Mini-Refraction Sonde development program demonstrated that an 85-gram sonde could be built using current technology. This second phase of the program was directed at determining the measurement accuracy of the minisonde. During this contract it has been demonstrated that the temperature and pressure sensors are capable of meeting an accuracy of 1°C and 2 millibars, respectively; in addition, measurements on the meteorological electronics show that they are capable of encoding and telemetering this accuracy.

The next phase of the program will consist of flight tests of the sondes built for this contract. Balloon-borne flights of the sonde will demonstrate field operation of the minisonde.